Biogeochemistry
https://doi.org/10.1007/s10533-018-0491-5

Iron sulfide formation on root surfaces controlled by the life cycle of wild rice (*Zizania palustris*)

Sophia LaFond-Hudson · Nathan W. Johnson · John Pastor · Brad Dewey

Received: 16 October 2017 / Accepted: 23 August 2018

Abstract Iron sulfide plaques have been observed on roots of wild rice (*Zizania palustris*) and other wetland plants grown in sulfur-impacted freshwater ecosystems, but the mechanism of their formation and ramifications for plants have not been investigated. We exposed a model annual wetland plant, *Zizania palustris*, to elevated sulfate concentrations (3.1 mM) and quantified the development of iron oxide and iron sulfide precipitates on root surfaces throughout the plant life cycle. During the onset of seed production, root surfaces amended with sulfate transitioned within 1 week from iron (hydr)oxide plaques to iron sulfide plaques. During the same week, Fe(III) decreased on roots of plants not amended with sulfate but FeS did not accumulate. Prior to FeS accumulation, sulfate-amended plants had taken up the same amount of N as unamended plants. After FeS accumulation, total plant nitrogen did not increase further on sulfate-amended plants, indicating a cessation in nitrogen uptake, whereas total plant N continued to increase in unamended plants. Sulfate-amended plants produced fewer and lighter seeds with less nitrogen than unamended plants. FeS precipitation on roots may be associated with elevated sulfide and inhibited nitrogen uptake before the end of the plant's life cycle, thus affecting the populations of this annual aquatic plant. We propose a mechanism by which a physiologically-induced decline in radial oxygen loss near the end of a plant's life cycle initiates a precipitous decline in redox potential at the root surface and in adjacent porewater, initiating accumulation of iron sulfide plaques. These plaques could be an important locus for iron sulfide accumulation in wetland sediments.

Keywords Root plaques · Radial oxygen loss · Iron–sulfur cycling · *Zizania palustris* · Electron accepting buffer

Responsible Editor: Charles T. Driscoll.

Electronic supplementary material The online version of this article (https://doi.org/10.1007/s10533-018-0491-5) contains supplementary material, which is available to authorized users.

S. LaFond-Hudson (✉)
Water Resource Science, University of Minnesota Duluth, Duluth, MN 55812, USA
e-mail: lafo0062@d.umn.edu

N. W. Johnson
Department of Civil Engineering, University of Minnesota Duluth, Duluth, MN 55812, USA
e-mail: nwjohnso@d.umn.edu

J. Pastor · B. Dewey
Department of Biology, University of Minnesota Duluth, Duluth, MN 55812, USA
e-mail: jpastor@d.umn.edu

B. Dewey
e-mail: bdewey@d.umn.edu

Published online: 11 September 2018

Introduction

Introduction of sulfate to low-sulfate freshwater ecosystems and subsequent reduction to sulfide can induce eutrophication, enhance methylmercury production, and decimate populations of sensitive aquatic plant species (Caraco et al. 1989; Gilmour et al. 1992; Smolders et al. 2003). Field observations have correlated elevated sulfide concentrations in sediment with population declines and decreased density of some aquatic plants (Myrbo et al. 2017; Pulido et al. 2012; Smolders et al. 2003). Black iron sulfide (FeS) plaques have been observed on the roots of aquatic plants grown with elevated sulfide in several sulfur addition experiments (Gao et al. 2003; Jacq et al. 1991; Koch and Mendelssohn 1989) including our outdoor mesocosm experiment with self-perpetuating wild rice (*Zizania palustris*) populations (Pastor et al. 2017); however, little is known about conditions conducive to iron sulfide precipitation on roots and the mechanism by which it occurs.

Roots of aquatic plants create redox interfaces that are hot spots for cycling of nitrogen, sulfur, iron, and other metals (Soana et al. 2015; Schmidt et al. 2011; Lee and McNaughton 2004). Many aquatic plants transport oxygen from the atmosphere to the roots through porous tissue called aerenchyma (Armstrong and Armstrong 2005). Radial oxygen loss from roots reacts with ferrous iron in sediment to form iron (hydr)oxide plaques at the interface of the oxidized root surface and the reduced sediment (Christensen and Sand-Jensen 1998; Mendelssohn and Postek 1982; Snowden and Wheeler 1995). Together, radial oxygen loss and iron (hydr)oxide plaques provide a supply of electron accepting compounds at the root surface, hereafter referred to as an electron accepting buffer. This buffer may inhibit sulfide formation and precipitation in several ways. The release of oxygen by plant roots may reoxidize sulfide and inhibit sulfate reduction (Holmer et al. 1998). In addition, Fe(III) can oxidize sulfide, and the reduction of Fe(III) to Fe(II) may outcompete sulfate reduction (Roden and Wetzel 1996; Hansel et al. 2015). Others have observed increased FeS precipitation on roots and in sediments shortly after plant senescence (Jacq et al. 1991; Giblin and Howarth 1984), suggesting a decrease in the strength of the electron accepting buffer. However, the timing of sulfide interactions with iron on root surfaces, particularly in relation to the life cycle of the plants, remains largely unexplored.

To explore these processes, we subjected wild rice, *Zizania palustris*, an annual plant that forms large monotypic stands in the lakes and rivers of Minnesota, Wisconsin, northern Michigan, and Ontario, to enhanced sulfate concentrations. Although radial oxygen loss has not been directly quantified in wild rice, aerenchyma tissue and root surface iron oxides have been studied and documented in this species (Stover 1928; Jorgenson et al. 2012). In a previous mesocosm experiment with wild rice, increasing concentrations of porewater sulfide decreased vegetative biomass production only slightly, but strongly decreased annual seed production, leading to population declines in subsequent years (Pastor et al. 2017). Hydroponics experiments have demonstrated that sulfide reduces nutrient uptake in wetland plants (Joshi et al. 1975; Koch and Mendelssohn 1989) through inhibition of metallo-enzymes in the electron transport chain and subsequent inhibition of ATP production required for nutrient transport (Allam and Hollis 1972; Koch et al. 1990; Martin and Maricle 2015). It is not well understood why the seed production life stage of wild rice is especially vulnerable to sulfide, but decreased seed production may be associated with the timing of favorable conditions for sulfate reduction and concomitant FeS accumulation on roots.

To identify the drivers of FeS formation on the root surfaces, we tested the hypothesis that surface water sulfate loading induces FeS formation on roots. To investigate the implications of FeS root plaques for nitrogen uptake during seed production, we explored the timing of FeS formation on wild rice roots. We exposed wild rice plants to elevated surface water sulfate and quantified the speciation of iron and sulfur on root surfaces and in rooting-zone porewater during reproductive life stages. Throughout the life cycle of the plant, we also monitored growth and seed production.

Methods

Sediment was collected from Rice Portage Lake (MN Lake ID 09003700, 46.703810, − 92.682921) on the Fond du Lac Band of Lake Superior Chippewa Reservation in Carlton County, Minnesota on 5/15/15 and placed in a 400 L polyethylene stock tank (High Country Plastics) where it was homogenized by

shovel. Initial total carbon in the sediment was 14.8 ± 1.70% and initial total nitrogen was 1.12 ± 0.13% by dry weight. Eighty 4 L plastic pails were then filled with 3 L of the sediment. Each 4 L pail was placed inside a 20 L bucket that was filled with 12 L of groundwater from an on-site well to provide a 12–15 cm water column. In each pail, two seeds that were harvested in 2014 from Swamp Lake on the Grand Portage Reservation (MN Lake ID 16000900, 47.951856, − 89.856844) were planted on 5/15/15 (Julian day 135).

Forty randomly chosen buckets were amended with sulfate and forty were left unamended. On 6/3/15, the forty amended buckets received an aliquot of stock solution (5.15 g of Na_2SO_4 dissolved in 200 mL of deionized water) to result in 300 mg L^{-1} (3.1 mM) sulfate. We hereafter refer to all porewater, sediment, and plants in these buckets as "amended". This concentration is close to the EPA secondary standard for drinking water, 250 mg L^{-1} (2.6 mM), intended to prevent laxative effects and an unpleasant taste. Although northeastern Minnesota generally has sulfate concentrations less than 10 mg L^{-1} (0.1 mM), concentrations of sulfate higher than 2.6 mM are found in some Minnesota waters, either naturally from geologic sources or from anthropogenic inputs (Myrbo et al. 2017). A sulfate concentration of 3.1 mM caused wild rice populations to go extinct within 5 years in previous mesocosm experiments with the same sediment (Pastor et al. 2017). The overlying water was sampled twice throughout the trial and re-adjusted to 3.1 mM SO_4 by adding additional Na_2SO_4 stock solution on 7/10/15. Unamended buckets had an average surface water sulfate concentration of 0.15 ± 0.01 mM when sampled on 6/23/15, consistent with the concentration of sulfate in groundwater from the on-site well. This is only slightly above observations of Moyle (1944) that wild rice grows best in waters less than 10 mg L^{-1} sulfate. We hereafter refer to all porewater, sediment, and plants in these buckets as "unamended." Shoots were thinned on 6/23/15 to one plant per bucket. Shoot height ranged from 10 to 20 cm and the tallest, most robust shoot in each bucket was left in place.

The annual life cycle of wild rice begins with emergence from the sediment and water column in June, continues with vegetative growth in July, followed by flowering and seed production in August, and ends with the shedding of seeds and death of the plant from late August to late September. Seeds overwinter in the sediment until they germinate in May (Grava and Raisanen 1978; Sims et al. 2012). Four plants were harvested every 2 weeks from randomly chosen amended and unamended buckets beginning at the onset of flowering (7/9/15, day 190) and continuing to the onset of seed production (8/20/15, day 232), after which plants were harvested weekly until senescence (9/22/15, day 265). The first seeds were collected on 8/20/15 (day 232) but were unripe and not yet filled. Mature seeds were not produced until 1 week after the start of seed production (day 239). On the last sample date (day 265) seeds were collected but were unfilled. Stems and leaves were no longer green, indicating that the plants had senesced. Of the four amended replicates sampled on this date, two plants did not produce seeds. Thus, "mature seed production" refers to seeds produced between Julian days 239–253.

Each plant was removed from the sediment and immediately rinsed in buckets of deoxygenated water continuously bubbled with a rapid stream of molecular nitrogen. If seeds were present, they were removed prior to sampling the plant and saved for separate analysis. While submerged in deoxygenated water, the stem was cut just above the root ball so that the shoots could be saved for mass and N analysis. The still submerged roots were then placed in jars full of deoxygenated water, which were immediately placed in a plastic bag flushed with molecular nitrogen and transported to an oxygen-free glove box (Coy Lab Products, 97.5% N_2, 2.5% H_2). In the glove box, the roots were cleaned of sediment and all organic matter except living wild rice roots prior to removing a 1–2 g section of wet root mass for acid volatile sulfide (AVS) and iron analysis.

The plants and seeds were rinsed with deionized water and dried in paper bags for 7 days at 65 °C. The dried plants were weighed, placed in polycarbonate vials with stainless steel balls, and shaken in a SPEX 800 M mixer mill until the samples were in a powdered form. Seeds were counted, weighed, and powdered using the same method. The samples were transferred to glass vials and dried again overnight at 65 °C with caps loosely covering the vials. Samples were quantified for total N on an elemental analyzer coupled to a Finnigan Delta Plus XP isotope ratio monitoring mass spectrometer.

Sediment was collected at the beginning and end of the growing season. Immediately after sediment homogenization (5/15/15), five replicate samples were placed in jars and analyzed for AVS and simultaneously extracted iron. At the end of the growing season (9/22/15), a 7 cm diameter sediment core was collected from the top 10 cm of each bucket prior to root sampling. Jars were filled completely with sediment and placed in a plastic bag filled with nitrogen to prevent oxidation during transport to a glove box. In the glove box, sediment was homogenized and allocated for AVS and iron extraction.

From both sediment and roots, AVS and iron were extracted simultaneously from a 1–3 g wet sample (0.1–0.5 g dry) using 7.5 mL 1 N HCl for 4 h using a modified diffusion method (Brouwer and Murphy 1994). During a room temperature acid incubation with gentle mixing, sulfide was trapped in an inner vial containing 3 mL Sulfide Antioxidant Buffer (SAOB) and subsequently quantified using a ThermoScientific sulfide ion-selective electrode with a detection limit of 0.01 mmol L^{-1}. After the extraction, two aliquots of the 1 N HCl extracts were used for iron quantification. Ferrous iron was immediately quantified colorimetrically using the phenanthroline method on a HACH DR5000 UV–Vis spectrophotometer (Greenberg et al. 1992), and weak acid extractable iron (sum of Fe(II) + Fe(III) concentrations, hereafter referred to as "total extractable iron") was quantified using a Varian fast sequential flame atomic absorption spectrometer with an acetylene torch.

A subset of roots was tested for chromium(II)-reducible sulfur (CRS) to determine whether AVS included all total reduced inorganic sulfur on the roots. A diffusion-based CRS method was used, which can fully extract all amorphous iron sulfide and pyrite and can partially extract elemental sulfur (Burton et al. 2008). The same sampling apparatus was used for extraction of AVS and CRS (see Burton et al. 2008 Fig. 1 for a diagram of the sampling apparatus). Chromic acid for CRS analysis was prepared according to Burton et al. (2008). Inside an oxygen-free glove box, a section of root from a plant previously analyzed for AVS was placed in the analysis bottle. An inner vial containing SAOB was also placed inside the bottle prior to sealing. Bottles were removed from the glove box and injected with chromic acid with no oxygen exposure. CRS was extracted for 48 h and quantified using a ThermoScientific sulfide ion-selective electrode.

One day prior to each root sampling date, the porewater was sampled for sulfide, sulfate, iron, and pH. First, pH was measured in situ with a ThermoScientific Orion pH electrode at a depth of 5 cm below the sediment surface and 2 cm from the stem of the wild rice plant. Porewater was collected using 5 cm length, 2 mm diameter tension lysimeter filters (Seeberg-Elverfeldt et al. 2005) (Rhizons) attached with a hypodermic needle to an evacuated, oxygen-free serum bottle sealed with a 20 mm thick butyl-rubber stopper (Bellco Glass, Inc). The entire filter end of the Rhizon was inserted vertically into the sediment just below the surface. The goal was to draw water from approximately the upper 5 cm of sediment without drawing surface water. The filter was placed with minimal jostling to avoid creating a cavity around the filter that would allow surface water to enter the sediment and contaminate the porewater. The Rhizon was placed approximately 2 cm away from the stem of the wild rice plant and on the opposite side from where pH was measured (Supplementary Fig. S1).

Porewater sulfide samples were drawn into 50-mL serum bottles preloaded with 0.2% 1 M ZnAc and 0.2% 6 M NaOH to preserve sulfide. Sulfide bottles were left to fill overnight, then stored at 4 °C in the sealed serum bottles used for sample collection for approximately 30 days before sulfide was quantified. Samples for porewater sulfate analysis were withdrawn from sulfide sampling bottles and filtered through a Dionex 1 cc metal cartridge and a 0.45 µm polyethersulfone filter approximately 3 months after they were collected. Porewater iron was collected in 8 mL serum bottles preloaded with 40% deionized water, 40% phenanthroline, 20% acetate buffer, and 1% concentrated hydrochloric acid. Iron bottles were filled until the solution turned light red, approximately 10 min. If the solution turned red before 8 mL were collected, samples were diluted with deionized water to bring the total solution to 8 mL. Iron samples were quantified within 2 h of sampling. Iron and sulfide in porewater were quantified colorimetrically using the phenanthroline and methylene blue methods, respectively, on a HACH DR5000 UV–Vis spectrophotometer (Greenberg et al. 1992). Sulfate was quantified using a Dionex ICS-1100 Integrated IC system (AS-DV Autosampler) (Greenberg et al. 1992). The saturation index was calculated to determine if the porewater was saturated with respect to iron sulfide (Eq. 1, $K_{sp} = 10^{-2.95}$)

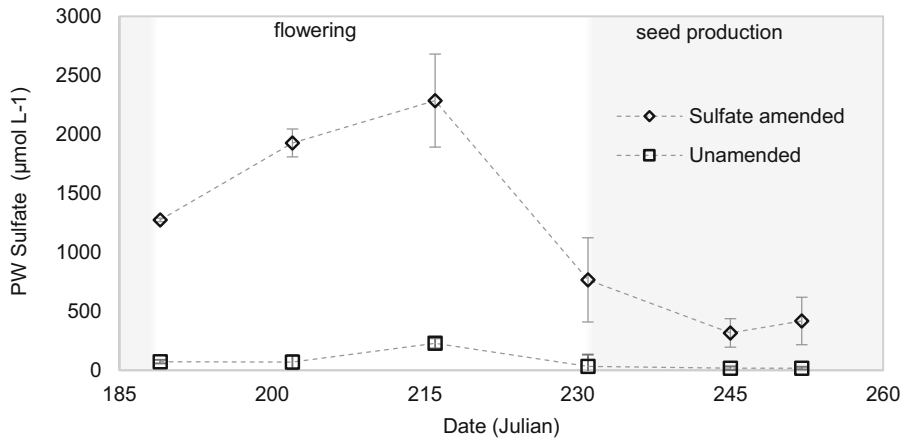

Fig. 1 Seasonal measurements of porewater sulfate concentrations 2 cm from the root surface. Diamonds depict amended plants while squares depict unamended plants. Error bars show one standard deviation around the mean. Shading represents different life stages. Shading on left side of figure represents pre-flowering, unshaded represents flowering, and shading on right represents seed production

(Stumm and Morgan 1996). A positive saturation index indicates oversaturation and a thermodynamic force to drive precipitation, and a negative value indicates undersaturation (and potential dissolution).

$$SI = \log \frac{[IAP]}{K_{sp}} \text{ where } IAP = \frac{[Fe^{2+}][HS^{-}]}{[H^{+}]} \quad (1)$$

Geochemical parameters and measured attributes of plants were analyzed using repeated measures analysis of variance to determine differences between amended and unamended treatments over the course of the growing season. Analyses were performed with a repeated measures ANOVA because although individual plants were harvested on each date, each sampling date was not independent of the prior sample dates. A paired *t* test was used to determine differences between AVS and CRS concentrations on subsamples from the same roots. Analyses were performed using the statistical software SAS. Logarithmic transformations were used when data was non-normal. Data are available at the Data Repository for the University of Minnesota (https://doi.org/10.13020/D68W98).

Results

Porewater sulfate and sulfide

Immediately before sulfate was added to amended buckets on Julian day 154, porewater sulfate concentrations were near 40 µmol L^{-1}. By the start of flowering (day 185), sulfate concentrations in amended porewater were over 1200 µmol L^{-1}, 30 times higher than the initial concentration (Fig. 1). Sulfate concentrations continued to rise for the first 30 days of flowering (until day 217), peaking at nearly 2300 µmol L^{-1}. Over a 4 week period (days 217–245) surrounding the onset of seed production, sulfate concentrations in amended porewater decreased by 86% to 315 µmol L^{-1}. Sulfate concentrations in unamended porewater were about 70 µmol L^{-1} at the start of flowering, roughly double the initial concentrations. Sulfate concentrations peaked at 230 µmol L^{-1} in unamended buckets on the same day as in amended buckets. During the same period that sulfate concentrations declined in amended porewater (days 217–245), sulfate concentrations in unamended buckets decreased by a similar proportion, 91%, to 20 µmol L^{-1}. Porewater sulfide did not differ between amended and unamended treatments (Supplementary Fig. S2). Concentrations averaged between 1 to 5 µmol L^{-1} during flowering and increased to an average of 8–17 umol L^{-1} at the start of seed production. Amended rhizospheres had a higher average sulfide concentration than unamended rhizospheres during seed production, but variability was high on the days porewater sulfide was elevated. Porewater sulfide concentrations decreased near the end of seed production and rose slightly at senescence.

Acid volatile sulfur on root surfaces

When grown in sediment with sulfate-amended overlying water (3.1 mM), amended plants developed a black coating on their root surfaces by the beginning of seed production on Julian day 231 (Fig. 2). The black precipitate started just above the root ball and extended along the entire length of the roots in the sediments. Adventitious roots that grew at the surface of the sediment, however, remained white, the natural color of wild rice root tissue. Unamended plants, grown in sediment with low concentrations of sulfate in overlying water (0.15 mM), developed amber coatings characteristic of iron (hydr)oxides over the same time period.

Roots of amended plants began accumulating AVS during the flowering stage (Julian days 190–230) of the life cycle (Fig. 3a). The rate of AVS accumulation abruptly accelerated during the seed production stage (days 231–252) from approximately 2 μmol g^{-1} day^{-1} to over 15 μmol g^{-1} day^{-1}. During the seed production stage, amended roots accumulated up to 100 times more AVS than unamended roots, reaching a maximum mean concentration of 298 ± 74 μmol g^{-1} dw at the end of seed production. In contrast, AVS on unamended roots remained at 3.2 ± 1.7 μmol g^{-1} dw throughout the season (Fig. 3b). Between the end of seed production and final senescence (day 265), AVS concentrations on amended roots remained elevated or decreased slightly.

Fig. 2 Sulfate-amended (left) and unamended (right) roots. Sulfate-amended (3.1 mM sulfate in surface water) root has black color extending from about 0.5 cm above the root ball down to the tips of the roots. Unamended (0.15 mM sulfate in surface water) root has amber color characteristic of iron (hydr)oxides, especially in the 2–3 cm below root ball. The photograph was taken during senescence in October, 2014 from a pilot experiment, but color is typical of roots in this experiment. (Color figure online)

Although AVS concentration in amended sediment increased by one order of magnitude over the life cycle (0.5–5 μmol g^{-1} dw, Supplementary Fig. S3), sediment contained approximately 50 times less AVS per gram than the roots. Concentrations of chromium reducible sulfur on both amended and unamended roots did not differ from AVS concentrations on the same roots during seed production, indicating that crystalline forms of FeS did not make up a significant proportion of reduced sulfur (paired t test, $p = 0.27, t = 0.63, n = 20$).

Iron speciation on root surfaces

During flowering, concentrations of Fe(III) and Fe(II) were similar between amended and unamended roots (Fig. 3). During seed production, the redox state of iron was altered by the presence of sulfate. Concentrations of Fe(II) were much higher on amended roots compared to unamended roots ($p < 0.001$, $F = 19.1$, $df = 1, 31$), despite no significant difference in concentrations of Fe(III) between treatments. During the first week of seed production (between days 232 and 239), the concentration of ferric iron on amended roots decreased by 86%, from 233 ± 135 to 31.7 ± 30.4 μmol g^{-1} dw while ferric iron on unamended roots decreased by 67%, from 438 ± 208 to 144 ± 131 μmol g^{-1} dw. This abrupt reduction of Fe(III) occurred the same week that the rate of net AVS accumulation increased on amended roots (Fig. 2). Following this transition, Fe(II) concentrations continued to increase (doubled) on amended roots but did not change on unamended roots.

Saturation index in porewater

Although the amended and unamended plants had significant differences in the speciation of solid-phase sulfur and iron on roots, the saturation index of FeS in the sediment porewater 2 cm away from the roots was

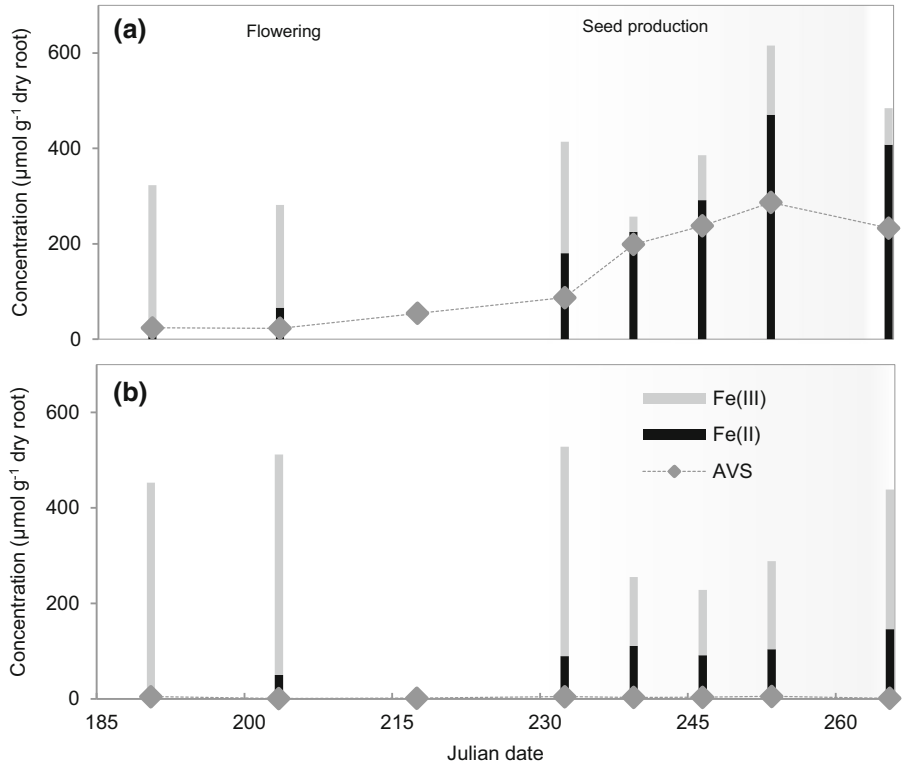

Fig. 3 Seasonal variations in iron speciation and root AVS for **a** sulfate-amended and **b** unamended conditions, and effective E_H on root surfaces. The gray bars in panels **a** and **b** indicate ferric iron and the black bars represents ferrous iron. Root AVS concentrations are shown by gray diamonds. Error bars are omitted for clarity, but standard deviation is on average 33% of the mean

not affected significantly by sulfate amendment (p = 0.177, F = 2.68, df = 1,4) and remained, on average, near zero but mostly negative ($-$ 1.4 $\pm$ 0.3 to 0.1 $\pm$ 1.0) throughout the life cycle (Supplementary Table S1).

Effects on plants

The transition of plants from the vegetative growth stage to the flowering and seed production stages of the life cycle coincided with the onset of a yellowing and senescence of leaves beginning the third week of August (around day 232). Amended plants, all of which developed FeS plaques on roots, produced fewer seeds (p = 0.067, F = 5.00, df = 1,6, Fig. 4) with less nitrogen (p = 0.052, F = 5.84, df = 1,6) and smaller mass (p = 0.069, F = 4.88, df = 1,6). During flowering, total plant N was similar between amended and unamended plants. But, during the subsequent seed production stage, total plant N continued to increase in the unamended plants, but not in the amended plants (p = 0.084, F = 4.27, df = 1,6).

Discussion

We observed rapid shifts in sulfur and iron speciation at the surface of wild rice roots during the plant life cycle that differed depending on sulfate amendment. At the onset of leaf senescence and seed production, sulfate concentrations in the porewater decreased. This was followed shortly by decreased Fe(III) concentrations on the root surface as well as increased, but highly variable, dissolved sulfide concentrations in porewater. At this stage, solid phase-sulfide sulfide increased clearly and consistently on roots of amended plants, but not on unamended plants. The rapid development of FeS plaques was concomitant with the development of fewer filled seeds with lower nitrogen contents. Total plant nitrogen continued to

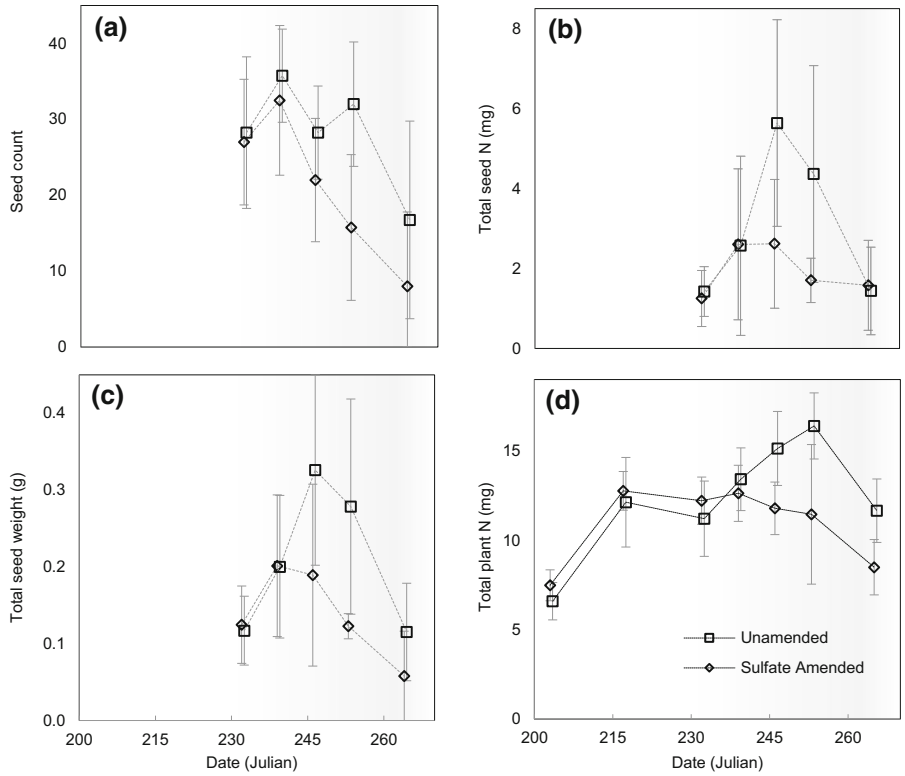

Fig. 4 Plant response in sulfate-amended and unamended conditions; **a** seed count. **b** Total seed mass. **c** Total mass of nitrogen in seeds, **d** total plant nitrogen, calculated by summing nitrogen from seeds, stems, and leaves. Diamonds represent plants grown in surface water with 3.1 mM sulfate and squares represent unamended plants. The shaded background represents the seed production life stage. Error bars represent one standard deviation of four replicates

increase in unamended plants but not in amended plants. The strong divergence between amended and unamended plants in total plant nitrogen and precipitation of FeS suggests a feedback between sulfur biogeochemistry on or near the root surface and plant nutrient uptake.

Sulfate amendments led to more reduced conditions and a more rapid development of iron sulfide precipitate on root surfaces, clearly confirming our hypothesis that surface water sulfate induces FeS accumulation on roots. In the absence of elevated sulfate, unamended plants filled out their seeds even when redox potential declined (Fig. 3, Supplementary Fig S4). In previous experiments with self-sustaining populations of wild rice (Pastor et al. 2017), elevated sulfate had little effect on total vegetative growth of adult plants but was associated with a decrease in the number and weights of seeds produced by mature plants at the late stages of the life cycle. FeS accumulates on roots during the last stages of wild rice's life cycle in which nitrogen taken up by the plant is allocated exclusively to panicles and seeds (Grava and Raisanen 1978; Sims et al. 2012). Porewater sulfide, which is known to decrease nitrogen uptake in plants, increased simultaneously with FeS on roots of amended plants. However, porewater sulfide was variable and increased in both amended and unamended rhizospheres, whereas FeS only increased on amended roots. Nitrogen uptake continued through the seed production phase of unamended plants but not in amended plants, which contained FeS plaques. FeS on roots may be a symptom of elevated porewater sulfide or further exacerbate its effects; our experiment was not able to distinguish between these possibilities. Regardless, the presence of root surface FeS strongly suggests that during seed production, a plant-induced reversal in the flow of electrons occurred: from a net flow of e-accepting capacity away from the root, sustaining Fe(III) in the rhizosphere, to a net flow of e- towards the root, reducing Fe(III) and introducing S(II).

The decline in nitrogen uptake and seed production concomitant with the initiation of FeS plaque precipitation on roots and porewater sulfide accumulation may explain the disproportionate effect of sulfate on seeds compared with its negligible effect on cumulative vegetative biomass prior to flowering and seed production. We suggest that plants are especially vulnerable to sulfide during seed production, because a seasonal decrease in root surface redox potential is compromised by further sulfide-induced depletion of the electron accepting buffer capacity of iron (hydr)oxides. The oxidation states of the amended and unamended root surfaces diverged during the transition from flowering to seed production (Supplementary Fig. S4), suggesting that root surface redox potential is, in part, controlled by a physiological mechanism tied to the plant's life cycle.

We hypothesize a pathway for how the living wild rice roots transition from iron (hydr)oxide plaques to iron sulfide plaques over the growing season (Fig. 5). Initially, conditions in the rooting zone are oxic, likely from radial oxygen loss (Fig. 5, stage [1]), as evidenced by precipitation of iron (hydr)oxides that accumulate equally on both amended and unamended root surfaces. At this initial stage, the root is protected from the electrons contained in sulfide and other reduced species by an ongoing supply of electron accepting inputs, composed of both oxygen from roots and iron (hydr)oxide coatings on roots (Holmer et al. 1998; Roden and Wetzel 1996). Sulfide encountering the iron (hydr)oxide buffer is oxidized or precipitates with iron while the electron accepting buffer is maintained. In amended conditions, some of this electron accepting buffer may be consumed (Fig. 5, stage [2]) during the flowering stage, allowing dissolved sulfide to penetrate nearer to the root surface. A decrease in radial oxygen loss near the onset of seed production, as vegetative growth ceases and leaves senesce, allows dissolved sulfide to reach the root surface. Sulfide exposure may further suppress radial oxygen loss by inducing suberization, the thickening of cell walls that prevents exchange of dissolved gases across the root (Armstrong and Armstrong 2005). After radial oxygen loss is suppressed, the electron accepting buffer capacity of iron (hydr)oxides can no longer be maintained and the remaining quantity of iron (hydr)oxides is then rapidly reduced due to a net decrease in the supply of electron acceptors to the rooting zone. A decrease in radial oxygen is likely tied to the end of the vegetative growth stage of the life cycle because both the amended and the unamended root surfaces simultaneously experience a loss of Fe(III) and a decline in porewater sulfate concentrations. Concentrations of

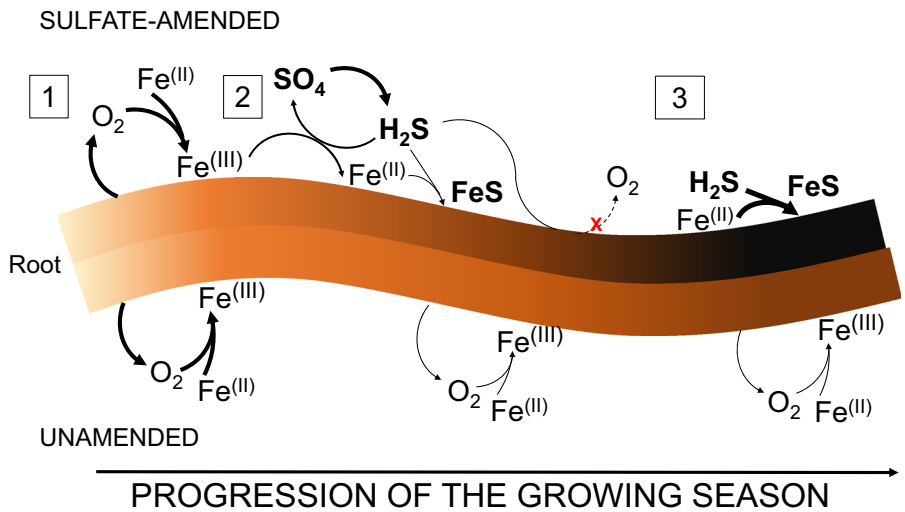

Fig. 5 Proposed mechanism of iron sulfide formation on wild rice roots exposed to elevated sulfate concentrations. Reactions depicted above the root occur on sulfate-amended root surfaces, and reactions depicted below the root occur on unamended root surfaces. Roots are protected by iron (hydr)oxides [1], but these iron (hydr)oxides are reduced by sulfide [2]. Exposure of roots to sulfide may induce suberization, the thickening of root cell walls, which leads to decreased radial oxygen loss. Root surface anoxia accelerates the precipitation of iron sulfides [3]. In unamended roots, radial oxygen loss creates iron (hydr)oxides that remain present the entire growing season but decrease slightly in response to the life-cycle. (Color figure online)

root Fe(III) and porewater sulfate remained low in unamended plants for the rest of the growing season. But, as the amended root surface shifts toward reducing conditions, sulfide almost exclusively precipitates with reduced iron rather than being re-oxidized (Fig. 5, stage [3]). In our amended buckets, rapid accumulation of root Fe(II), root AVS, and porewater sulfide occurred within a 1–2 week period during seed production immediately following the precipitous decline of porewater sulfate and root surface Fe(III). In unamended buckets, root Fe(II) and AVS did not accumulate further, and while porewater sulfide increased, it was highly variable.

The most likely explanation for a redox transition at both the unamended and amended roots is a decrease in radial oxygen loss at the end of the vegetative growth stage when the leaves begin to senesce. Many mechanisms of rhizosphere oxidation have been described, including diffusion of atmospheric oxygen (Armstrong 1980), advection induced by temperature and vapor gradients (Dacey 1980) and Venturi-induced convection (Armstrong et al. 1992). Several studies have observed a correlation between light and rhizosphere oxygenation on diurnal time scales (Lee and Dunton 2000; Pedersen et al. 2004; Jensen et al. 2005), suggesting that some, if not most, radial oxygen loss may be photosynthetically derived. It has been previously suggested that accumulation of FeS occurs on white rice (*Oryza sativa*) roots only after plant senescence because dead roots no longer oxidize the rhizosphere (Jacq et al. 1991). However, as the plant approaches senescence, oxygen transport to the roots may decrease due to lower photosynthesis rates, subsequently slowing the regeneration of the electron accepting buffer of the root surface (Biswas and Choudhuri 1980). We observed a decrease in redox around the time that plants started to yellow and show early signs of senescence, consistent with a life-cycle-induced decline in radial oxygen loss.

Despite the rapid accumulation of FeS on roots in amended plants, the saturation index in sediment 2 cm from the roots remained relatively low, suggesting that the most severe decline in redox potential was confined to near the root surface. The Fe(II) in the FeS plaques may have come from the reduction of iron (hydr)oxides previously accumulated on the root surface. On the other hand, the sulfide in FeS plaques must have been supplied from a source external to the root. Although experimental conditions may have impacted the timing of sulfate intrusion to the rooting zone, porewater sulfate concentrations were already well above the half saturation constant for biological sulfate reduction at the start of flowering (Pallud and Van Cappellen 2006), making it unlikely that the redox transition occurred from a delay in sulfate availability and reduction at the root surface. Once leaf senescence began, porewater sulfate concentrations ($\sim$ 2000 μmol L^{-1}) declined by more than 80% followed by rapid accumulation of porewater sulfide (from $\sim$ 2 to 12 μmol L^{-1}) and AVS on the root surfaces ($\sim$ 300 μmol g^{-1}). Adjacent porewater sulfide was relatively low compared to the amount of sulfur in the porewater sulfate and root AVS pools. This suggests that a large amount of sulfur passes through the porewater sulfide pool very quickly, a scenario consistent with our proposed mechanism by which sulfide near the root surface is either oxidized by the electron accepting buffer or precipitated with Fe(II). Sediment AVS (5 μmol g^{-1}) was a larger component of overall solid-phase S accumulation due to its larger mass, but did not, apparently, experience the concentrated introduction of sulfide in the same way as roots. The rapid and concentrated accumulation of iron sulfide on roots in the setting of undersaturated porewater suggests an overwhelmingly plant-dominated geochemical niche very close to the root surface.

Beyond affecting wild rice populations, the mechanism behind the rapid accumulation of FeS on roots has implications for the fate of iron and sulfide in wetland sediments. Vegetated sediment in white rice paddies (Jacq et al. 1991) and in riparian wetlands containing *Phragmites australis* and *Zizania latifolia* (Choi et al. 2006) has higher concentrations of FeS than non-vegetated sediment. Significant accumulation of FeS on white rice roots has been observed after senescence (Jacq et al. 1991), likely because decaying root material stimulates iron and sulfate reduction. When roots coated with FeS decompose, the FeS becomes incorporated into the bulk sediment. Due to the concentrated introduction of both electron donors and acceptors to the subsurface, each generation of an annual plant is effectively a "pump" for the incorporation of FeS precipitate into the sediment. In dense stands of aquatic plants, annual contributions of FeS from roots could significantly alter the geochemistry of the sediment within years to decades. If FeS plaques occur concomitantly with population declines in

wetland plants, the plant-induced sulfur pump may only last a few generations but would have implications for changes in species composition in wetland plant communities. Understanding the rates of the distinctly plant-induced sulfur pump and the short- and long- term interactions of near-root processes with bulk sediment could help to predict how the distribution of wetland vegetation and sulfur accumulation change in response to a perturbation in surface water sulfate concentrations.

The results of this study may provide a mechanistic link between observed sulfide toxicity in lab hydroponic experiments (Koch et al. 1990; Koch and Mendelssohn 1989; Pastor et al. 2017) and empirical evidence of sulfur-induced population declines of wetland plants (Lamers et al. 2002; Myrbo et al. 2017; Pastor et al. 2017; Pulido et al. 2012; Smolders et al. 2003). Our observation that sulfur cycling is altered *during* the life cycle rather than after senescence allows for the possibility of rapid feedbacks between sediment and porewater geochemistry on the one hand and annual plant populations on the other. Understanding the timing of when electron accepting buffers are present or absent and how that correlates with the plant life cycle can provide insight into how populations of wild rice and other aquatic plant species will respond to perturbations in sulfur loading to ecosystems.

Acknowledgements This research was funded by Minnesota Sea Grant and Fond du Lac Band of Lake Superior Chippewa. Sediment was provided from a wild rice lake on the Fond du Lac Reservation.

Author contributions SL-H and BD collected and analyzed samples. SL-H performed statistical analyses with guidance from JP. All authors contributed to interpreting the data and writing the manuscript.

Compliance with ethical standards

Conflict of interest The authors declare no competing financial interests.

References

Allam A, Hollis J (1972) Sulfide inhibition of oxidases in rice roots. Phytopathology 62:634–639

Armstrong W (1980) Aeration in higher plants. In: Andrews JH, Tommerup IC (eds) *Advances in botanical research*. Academic Press, Boca Raton, pp 225–332

Armstrong J, Armstrong W (2005) Rice: sulfide-induced barriers to root radial oxygen loss, Fe^{2+} and water uptake, and lateral root emergence. Ann Bot 96:625–638. https://doi.org/10.1093/aob/mci215

Armstrong J, Armstrong W, Beckett P (1992) *Phragmites australis*: venturi and humidity induced pressure flows enhance rhizome aeration and rhizosphere oxidation. New Phytol 120(2):197–207

Biswas AK, Choudhuri MA (1980) Mechanism of monocarpic senescence in rice. Plant Physiol 65:340

Brouwer H, Murphy T (1994) Diffusion method for the determination of acid-volatile sulfides (Avs) in sediment. Environ Toxicol Chem 13(8):1273–1275. https://doi.org/10.1897/1552-8618(1994)13[1273:DMFTDO]2.0.CO;2

Burton ED, Sullivan LA, Bush RT, Johnston SG, Keene AF (2008) A simple and inexpensive chromium-reducible sulfur method for acid-sulfate soils. Appl Geochem 23:2759–2766. https://doi.org/10.1016/j.apgeochem.2008.07.007

Caraco N, Cole J, Likens G (1989) Evidence for sulphate-controlled phosphorus release from sediments of aquatic systems. Nature 341(6240):316

Choi J, Park S, Jaffe P (2006) The effect of emergent macrophytes on the dynamics of sulfur species and trace metals in wetland sediments. Environ Pollut 140:286–293. https://doi.org/10.1016/j.envpol.2005.07.009

Christensen K, Sand-Jensen K (1998) Precipitated iron and manganese plaques restrict root uptake of phosphorus in *Lobelia dortmanna*. Can J Bot 76:2158–2163

Dacey J (1980) Internal winds in water lilies: an adaptation for life in anaerobic sediments. Science 210(4473):1017–1019

Gao S, Tanji K, Scardaci S (2003) Incorporating straw may induce sulfide toxicity in paddy rice. Calif Agric 57(2):55–59

Giblin A, Howarth R (1984) Porewater evidence for a dynamic sedimentary iron cycle in salt marshes. Limnol Oceanogr 29(1):47–63

Gilmour C, Henry E, Mitchell R (1992) Sulfate stimulation of mercury methylation in freshwater sediments. Environ Sci Technol 26(11):2281–2287

Grava J, Raisanen K (1978) Growth and nutrient accumulation and distribution in wild rice. Agron J 70:1077–1081

Greenberg AE, Clesceri LS, Eaton AD (1992) Standard methods for the examination of water and wastewater. American Public Health Association, Washington, DC

Hansel C, Lentini C, Tang Y, Johnston D, Wankel S, Jardine P (2015) Dominance of sulfur-fueled iron oxide reduction in low-sulfate freshwater sediments. ISME J 9(11):2400

Holmer M, Jensen HS, Christensen KK, Wigand C, Andersen FØ (1998) Sulfate reduction in lake sediments inhabited by the isoetid macrophytes *Littorella uniflora* and *Isoetes lacustris*. Aquat Bot 60:307–324

Jacq VA, Prade K, Ottow JCG (1991) Iron sulphide accumulation in the rhizosphere of wetland rice (*Oryza sativa* L.) as the result of microbial activities. Dev Geochem 6:453–468

Jensen S, Kühl M, Glud R, Jørgensen L, Priemé A (2005) Oxic microzones and radial oxygen loss from roots of Zostera marina. Mar Ecol Prog Ser 293:49–58

Jorgenson K, Lee P, Kanavillil N (2012) Ecological relationships of wild rice, Zizania spp. 11. Electron microscopy

study of iron plaques on the roots of northern wild rice (*Zizania palustris*). Botany 91(3):189–201

Joshi M, Ibrahim I, Hollis J (1975) Hydrogen sulfide: effects on the physiology of rice plants and relation to straighthead disease. Phytopathology 65:1165–1170

Koch MS, Mendelssohn I (1989) Sulphide as a soil phytotoxin: differential responses in two marsh species. J Ecol 77(2):565–578

Koch MS, Mendelssohn IA, McKee KL (1990) Mechanism for the hydrogen sulfide-induced growth limitation in wetland macrophytes. Limnol Oceanogr 35(2):399–408

Lamers L, Falla S, Samborska E, van Dulken L, van Hengstum G, Roelofs J (2002) Factors controlling the extent of eutrophication and toxicity in sulfate-polluted freshwater wetlands. Limnol Oceanogr 47(2):585–593

Lee K, Dunton KH (2000) Diurnal changes in pore water sulfide concentrations in the seagrass *Thalassia testudinum* beds: the effects of seagrasses on sulfide dynamics. J Exp Mar Biol Ecol 255:201–214

Lee PF, McNaughton KA (2004) Macrophyte induced microchemical changes in the water column of a northern Boreal Lake. Hydrobiologia 522(1–3):207–220

Martin NM, Maricle BR (2015) Species-specific enzymatic tolerance of sulfide toxicity in plant roots. Plant Physiol Biochem 88:36–41. https://doi.org/10.1016/j.plaphy.2015.01.007

Mendelssohn IA, Postek MT (1982) Elemental analysis of deposits on the roots of *Spartina alterniflora* Loisel. Am J Bot 69(6):904–912

Moyle J (1944) Wild rice in Minnesota. J Wildl Manag 8(3):177–184

Myrbo A, Swain EB, Engstrom DR, Coleman Wasik J, Brenner J, Dykhuizen Shore M, Blaha G (2017) Sulfide generated by sulfate reduction is a primary controller of the occurrence of wild rice (*Zizania palustris*) in shallow aquatic ecosystems. J Geophys Res 122(11):2736–2753

Pallud C, Van Cappellen P (2006) Kinetics of microbial sulfate reduction in estuarine sediments. Geochim Cosmochim Acta 70(5):1148–1162

Pastor J, Dewey B, Johnson NW, Swain EB, Monson P, Peters EB, Myrbo A (2017) Effects of sulfate and sulfide on the life cycle of *Zizania palustris* in hydroponic and mesocosm experiments. Ecol Appl 27(1):321–336

Pedersen O, Binzer T, Borum J (2004) Sulphide intrusion in eelgrass (*Zostera marina* L.). Plant Cell Environ 27(5):595–602

Pulido C, Keijsers DJ, Lucassen EC, Pedersen O, Roelofs JG (2012) Elevated alkalinity and sulfate adversely affect the aquatic macrophyte *Lobelia dortmanna*. Aquat Ecol 46:283–295

Roden EE, Wetzel RG (1996) Organic carbon oxidation and suppression of methane production by microbial Fe(III) oxide reduction in vegetated and unvegetated freshwater wetland sediments. Limnol Oceanogr 41(8):1733–1748

Schmidt H, Eickhorst T, Tippkoetter R (2011) Monitoring of root growth and redox conditions in paddy soil rhizotrons by redox electrodes and image analysis. Plant Soil 341:221–232. https://doi.org/10.1007/s11104-010-0637-2

Seeberg-Elverfeldt J, Schlüter M, Feseker T, Kölling M (2005) Rhizon sampling of porewaters near the sediment-water interface of aquatic systems. Limnol Oceanogr 3(8):361–371

Sims L, Pastor J, Lee T, Dewey B (2012) Nitrogen, phosphorus, and light effects on growth and allocation of biomass and nutrient in wild rice. Oecologia 170:65–76

Smolders A, Lamers L, den Hartog C, Roelofs J (2003) Mechanisms involved in the decline of *Stratiotes aloides* L. in The Netherlands: sulphate as a key variable. Hydrobiologia 506(1–3):603–610. https://doi.org/10.1023/B:HYDR.0000008551.56661.8e

Snowden R, Wheeler B (1995) Chemical changes in selected wetland plant species with increasing Fe supply, with specific reference to root precipitates and Fe tolerance. New Phytol 131:503–520. https://doi.org/10.1111/j.1469-8137.1995.tb03087.x

Soana E, Naldi M, Bonaglia S, Racchetti E, Castaldelli G, Brüchert V, Viaroli P, Bartoli M (2015) Benthic nitrogen metabolism in a macrophyte meadow (*Vallisneria spiralis* L.) under increasing sedimentary organic matter loads. Biogeochemistry 124(1–3):387–404

Stover E (1928) The roots of wild rice *Zizania Aquatica* L. Ohio J Sci 28(1):43–49

Stumm W, Morgan JJ (1996) Chemical equilibria and rates in natural waters. Aquatic chemistry. Wiley, New Jersey

Aquatic Botany 164 (2020) 103230

Contents lists available at ScienceDirect

Aquatic Botany

journal homepage: www.elsevier.com/locate/aquabot

Interactions between sulfide and reproductive phenology of an annual aquatic plant, wild rice (*Zizania palustris*)

Sophia LaFond-Hudson[a,*], Nathan W. Johnson[a], John Pastor[b], Brad Dewey[b]

[a] Department of Civil Engineering, University of MN Duluth, 221 SCiv, 1405 University Drive, Duluth, MN, 55812, USA
[b] Department of Biology, University of MN Duluth, 207 SSB, 1035 Kirby Drive, Duluth, MN, 55812, USA

ARTICLE INFO

Keywords:
Ontogeny
Geochemistry
Wild rice
Seed production
Rhizosphere

ABSTRACT

Aquatic plants live in anoxic sediments that favor formation of hydrogen sulfide, a known phytotoxin. We investigated how the phenology of reproductive life stages of wild rice (*Zizania palustris* Poaceae), an annual aquatic graminoid, is influenced by rooting zone sulfur geochemistry in response to elevated sulfate and sulfide. In addition, we characterized how redox conditions in the rooting zone change throughout reproduction to determine if they are tied to plant life stage. The redox conditions in sediment decreased just prior to flowering, and again just prior to seed production for all plants, allowing sulfide to accumulate at the root surface of sulfate-amended plants. Plants exposed to sulfide initiated seed production later than unamended plants. Sulfide appears to slow plant development in a way that gives the plant less time to allocate nutrients to seeds before senescence. The impact of sulfide in delaying reproductive life stages of wild rice and changing seasonal rooting zone biogeochemistry could extend to other plant species and additional chemical species that change mobility with redox potential, such as phosphate, manganese, mercury, and other metals.

1. Introduction

Many aquatic plants grow in sediments with low redox potential that favors formation of toxic reduced compounds like sulfide. To cope with these conditions, some aquatic plants transport oxygen to the roots through hollow aerenchyma tissue, release it into the rhizosphere, and form iron oxide plaques on root surfaces (Stover, 1928; Mendelssohn et al., 1995; Colmer, 2003; Jorgenson et al., 2012). The released oxygen and iron oxides may protect roots from dissolved sulfide species (Trolldenier, 1988; Van der Welle et al., 2007; Schmidt et al., 2011; Soana and Bartoli, 2013). Many wetland plants, including wild rice, are vulnerable to dissolved sulfide (Koch and Mendelssohn, 1989; Carlson et al., 1994; Lamers et al. 1998; Pastor et al., 2017). Wild rice (*Zizania palustris*, Poaceae), an annual aquatic graminoid which forms large monotypic stands in lakes of the Western Lake Superior region, is especially sensitive during the seedling and seed production life stages, suggesting that the ability to withstand sulfide varies throughout their life cycle (Pastor et al., 2017; LaFond-Hudson et al., 2018).

Plants growing in nutrient-limited conditions sometimes experience ontogenetic drift, a phenomenon in which morphological development through successive life stages is slowed (McConnaughay and Coleman, 1999; Sims et al., 2012). Because the allocation of biomass to different tissues changes throughout a plant's life cycle, delayed development has sometimes been misdiagnosed as morphological plasticity in experiments in which plants are normalized by date or age, rather than size or life stage (Coleman et al., 1994). Nitrogen is the limiting nutrient to wild rice (Sims et al., 2012) and its uptake is tied to specific life stages (Grava and Raisanen, 1978). About 30 % of nitrogen is taken up during early vegetative growth, 50 % is taken up during the growth of the stem until flowering, and 20 % is taken up during seed production (Grava and Raisanen, 1978). Dissolved sulfide inhibits nutrient uptake (Allam and Hollis, 1972; Koch et al., 1990; Martin and Maricle, 2015). If nitrogen uptake in wild rice is inhibited or slowed by sulfide, it may slow the rate at which the plant progresses through subsequent life stages and limit the quantity of N uptake available for seed production.

Near the end of an annual plant's life cycle when plants allocate resources from leaves into flowers and seeds, photosynthesis declines and radial oxygen loss from roots may also decrease, creating favorable conditions for reduction of iron oxides and sulfate (Schmidt et al., 2011). Several mechanisms for maintaining radial oxygen loss from roots have been described, including pressure gradients that actively pump oxygen from new leaves, through roots, to old leaves (Dacey, 1980; Armstrong, 1980; Armstrong et al., 1992); and production and transport as a byproduct of photosynthesis (Marzocchi et al., 2019).

* Corresponding author.
E-mail addresses: lafo0062@d.umn.edu (S. LaFond-Hudson), nwjohnso@d.umn.edu (N.W. Johnson), jpastor@d.umn.edu (J. Pastor), bdewey@d.umn.edu (B. Dewey).

https://doi.org/10.1016/j.aquabot.2020.103230
Received 11 December 2019; Received in revised form 14 February 2020; Accepted 18 February 2020
Available online 24 February 2020

Table 1
Descriptions of the life stages of wild rice and the range of dates for each life stage in which at least one *Zizania palustris* plant was observed (initially $n = 64$, followed by incrementally smaller sample sizes due to destructive sampling). Ranges are described for plants grown in water amended with 300 mg L^{-1} sodium sulfate or grown in water unamended, with background sulfate concentrations of ~8-14 mg L^{-1}. Life stages 1 through 3 pertain to seedling and early emergent stages that did not develop iron sulfide plaques on roots. Designation and description of life stages from Grava and Raisanen (1978) and Sims et al. (2012).

Lifestage Name	Lifestage Number	Characteristics	Dates Observed	
			Amended	Unamended
Mid tillering	4	Tiller (main stem) grows more than one leaf	210-235	210-222
Jointing	5	Internodes elongate	210-240	210-240
Boot	6	Panicles emerge from stems	235-249	235-245
Early flowering	7	A few flowers bloom, some not yet emerged	235-245	235-245
Mid flowering	8	Most flowers bloom	235-249	235-245
Late flowering	9	Most panicles empty, few flowers still bloom	235-249	235-249
Seed production	10	Seed hull develops, seed filling occurs	240-263	235-263
Seed maturity	11	Filled, ripe seeds present, a few dropped	255-263	255-263
Senescence	12	All seeds dropped, green tissues disappear	280	280

Although the exact mechanism of radial oxygen loss in wild rice is not yet known, the aforementioned mechanisms may be inhibited by the senescence of leaves during reproduction. We previously reported a decline in the redox potential of root surfaces during the seed production life stage (LaFond-Hudson et al., 2018). In plants grown in sediment without sulfur amendment, iron oxide plaques on root surfaces decreased, but in sulfate-amended plants, iron oxide plaques transitioned to iron sulfide, which further accumulated on root surfaces and coincided with production of fewer, smaller seeds with less nitrogen relative to unamended plants. In plants exposed to sulfide, the total uptake of nitrogen ceased during the onset of iron sulfide plaque formation and thickening while unamended plants continued to accumulate nitrogen in seeds (LaFond-Hudson et al., 2018). In this paper, we specifically explore the relationship between sulfur geochemistry and phenology of life stages, as both may control each other through interactions that culminate in the redox potential of root surfaces. We use wild rice (*Zizania palustris,* Poaceae) as our model organism to investigate connections between sulfide and iron geochemistry in the rhizosphere and reproductive phenology and ontogeny. Because wild rice is an annual plant, the ontogeny of development is equivalent to the annual phenology. So in this case, the two words are synonymous, except that ontogeny has the connotation of development whereas phenology has the connotation of seasonality.

Wild rice is a culturally, economically, and ecologically important macrophyte that is harvested for its grain (Fond du Lac Band of Lake Superior Chippewa, 2018). An advantage of using an annual plant is the relatively simple life cycle; root and shoot growth starts over each year, photosynthesis declines and vegetative structures senesce during the transition from vegetative to reproductive life stages, and seeds are produced at the end of the growing season just prior to death. In addition, standard markers of transitions in life cycle stages for wild rice have been established in prior research in the context of nutrient limitation (Grava and Raisanen, 1978; Sims et al., 2012).

Motivated by acute and population-level impacts of sulfide on aquatic plants, we compare the ontogenetic progression of life stages with the development of iron sulfide plaques throughout the life cycle of wild rice. Sulfide may slow ontogenetic development, but plant life stage may in turn control rhizosphere redox conditions and the amount of sulfur present as reactive sulfide. To investigate these geochemical and phenological interactions, we quantify the timing and length of life stages and seed production along with the concurrent accumulation of iron sulfide plaques.

2. Methods

2.1. Experimental design

Individual wild rice plants were grown outside in polyethylene buckets, 32 of which were amended with 300 mg L^{-1} sulfate and 32 of which were left unamended. Although many lakes and rivers in central and northern Minnesota have concentrations of sulfate lower than 10 mg L^{-1}, several current and former wild rice lakes and rivers have sulfate concentrations near or above 300 mg L^{-1}. Additionally, 300 mg L^{-1} is close to the EPA secondary standard for drinking water and is a concentration we have used in several prior sulfate-addition experiments with wild rice. Sediment was collected on 01-Jun-2016 from Rice Portage Lake (MN Lake ID 09003700, 46.7038, -92.6829) on the Fond du Lac Band of Lake Superior Chippewa Reservation in Carlton County, Minnesota. This lake is a productive and unpolluted wild rice lake with little or no settlement along its shores and its sediment is organic-rich mud. The sediment was not sieved, but thoroughly homogenized and loaded into 4 L plastic pails that were set inside 12 L buckets (see LaFond-Hudson et al., 2018) on 25-Jun-2016. Water was added from a nearby well (sulfate concentration ranging from 8 to 14 mg L^{-1}) to provide a 12 − 15 cm water column. Two wild rice seeds obtained from Rice Portage Lake were planted in each bucket on 26-Jun-2016 (Julian day 177). All buckets had at least one seedling by 28-Jun-2016 (day 179), and the lesser robust plant of the two was removed a week later. Half of the buckets had sodium sulfate added on 28-Jun-2016 and 05-Aug-2016 (days 179, 217) to maintain surface water sulfate concentrations of 300 mg L^{-1}. Plants remained outside for the entire duration of the experiment. Further details on the maintenance of buckets can be found in LaFond-Hudson et al. (2018).

2.2. Sampling methods

To compare changes in pace of progressions through the life cycle, we examined initiation of life stages from a subset of plants that completed their entire life cycle through seed production. We define initiation as the first date a plant was observed to be in a life stage. Life stages were identified visually and nondestructively according to the descriptions codified by Grava and Raisanen (1978) and further subdivided by Sims et al. (2012).

Our observations of the phenology of wild rice began with mid tillering, a life stage in which the main stem, the tiller, grows more than one leaf above the surface of the water (Table 1). Prior life stages include emergence of the seedling from sediment (life stage 0), the floating leaf stage (life stage 1), the first aerial leaf (life stage 2), and the formation of the tiller, the main stem that will eventually produce flowers and seeds (life stage 3). We started observations with mid tillering (life stage 4) because it is the last vegetative growth stage before reproductive life stages. After mid tillering, the internodes of the tiller elongate (jointing, life stage 5) and the panicles emerge (boot, life stage 6) in preparation for flowering (life stages 7–9). Flowering is broken into early (7), mid (8), and late (9) flowering by the proportion of flowers emerged and blooming. Once flowers have finished blooming, a

seed hull develops and seed production begins (life stage 10). Filled seeds start to drop once they reach maturity (life stage 11), and senescence is reached once all seeds have dropped and leaves have turned completely yellow (life stage 12). Life stages of each plant and date were recorded eight times during the growing season.

When at least half of the plants were in a specific life stage, four sulfate-amended plants and four unamended plants in that life stage were destructively harvested to determine root surface geochemistry. When the plants entered the seed production life stage, harvests were made on three separate dates, each approximately a week apart, spanning the duration of the seed production life stage. Sampling at a more frequent temporal resolution during seed production enabled us to make detailed observations of the accumulation of iron sulfide (or lack thereof) on the roots during a potentially critical time for sulfide exposure.

2.3. Biological and chemical analysis

On each sampling date, the same eight plants that were harvested were separated into aboveground vegetative tissue, seed tissue, and root tissue according to LaFond-Hudson et al. (2018). Vegetative tissue and seed tissues were dried for seven days at 65 °C and weighed. Total N concentrations were determined with a Thermo Electron Flash EA 1112 CHNS Analyzer. Fresh roots were analyzed for acid volatile sulfide (AVS) and weak acid extractable iron the same day plants were harvested, taking great care to avoid exposure to oxygen (LaFond-Hudson et al., 2018). Iron and acid volatile sulfur (AVS) were simultaneously extracted from entire roots using 1 M deoxygenated HCl for four hours. AVS was volatilized and trapped in a sulfide antioxidant buffer (SAOB) using a modified diffusion method (Brouwer and Murphy, 1994). AVS was quantified using a sulfide-selective electrode. Iron was extracted into the 1 M HCl and analyzed for total extractable iron and Fe(II). Fe (III) was estimated from the difference between total iron and Fe(II). Total iron was quantified using a Varian fast sequential flame atomic absorbance spectrometer with an acetylene torch. Fe(II) was quantified on the day of extraction using the phenanthroline method on the spectrophotometer. After extraction, roots were dried at 38 °C for 24 h to determine dry mass.

2.4. Data analysis

Data are publicly available in the Data Repository of University of Minnesota (DRUM) and can be accessed at https://conservancy.umn.edu/handle/11299/208579. We used a two-sample *t*-test to compare differences between sulfate-amended and unamended conditions for seed measurements and root sulfide. Because we sampled destructively to measure root surface sulfide and iron, dates for the initiation of early reproductive life stages contain a larger sample size relative to the seed production life stage. Conclusions about the initiation of life stages between treatments are based only on the subset of plants that reached seed production in this experiment, and thus are not influenced by changes in sample size. For this subset of plants, we calculate the cumulative distribution of the date on which each life stage was initiated by summing the number of plants that are at or beyond the life stage. We also calculated the duration of seed stage for each plant in this subset using the difference between the first day we observed filled seeds and the first day we observed dropped or missing seeds. In many plants, seed production ended artificially early due to our destructive sampling design. In these cases, we used the harvest date as the end date in our calculation of duration and refer to the resulting value as "experimental duration". We investigated correlations between experimental duration and yield of seed production (seed count, seedhead mass, and seedhead nitrogen mass) to understand progression in seed development within the seed production life stage. We used these linear relationships to infer the seed yield at "true duration", which we define as the probable duration of seed production if plants were not harvested. For true duration, we use the average last date seeds were observed in parallel wild rice experiments. These parallel experiments occurred in the same year, used the same sediment and tested sulfate-addition but did not use destructive sampling (Table S1).

The effective redox potential at the root surface was calculated using a modified Nernst equation (Stumm and Morgan, 2012).

$$p\varepsilon = p\varepsilon^{\circ} + \frac{1}{n} log \frac{\{ox\}}{\{red\}} \quad (1)$$

$$p\varepsilon = 16 - 3pH + log \frac{\{Fe(III)\}}{\{Fe(II)\}} \quad (2)$$

$$E_h^* = \frac{2.3RTp\varepsilon}{F} \quad (3)$$

While not strictly representative of the activity in solution, we use root surface Fe(III) and Fe(II) as a proxy for the activity of oxidized and reduced Fe in the rooting zone. Because the system is dynamic, root surface (solid-phase) quantities likely mirror the activity of iron in solution enough to draw general conclusions about the direction of the flow of electrons.

3. Results

3.1. Sulfide effects on phenology

When life stage observations began (Julian day 210), unamended plants were ahead by nearly a full life stage (mean life stage of 4.5 ± 0.5 unamended compared with mean life stage of 3.8 ± 0.6 amended, $p < 0.01$, two-sample t test), indicating that vegetative growth life stages were delayed by sulfate amendment. Most amended plants initiated jointing later than unamended plants (mean Julian day 217 ± 9 unamended, mean Julian day 226 ± 9 amended, $p = 0.005$, $n = 17$), but both treatments initiated the boot stage at similar times (mean Julian day 237 ± 3 for both, Fig. 1a, b). Because the boot stage occurs quickly, our temporal resolution may not have captured any differences in timing if they existed. From days 220–235, about half of the unamended plants initiated mid flowering, compared to only a quarter of amended plants (Fig. 1c). During the same time frame, one third of unamended plants initiated seed production, compared to no amended plants (Fig. 1d). Eight days later, day 243, a comparable number of amended plants entered seed production. Amended plants entered seed production during a narrower range of time, with ~75 % of plants reaching this life stage between days 240–250 (mean Julian day 247 ± 5), while the initiation of seed production was spread over a 2 week window for unamended plants (244 ± 7 days). Due to the destructive sampling required by our experimental design, we were unable to quantify the end date of seed production in this experiment, but we estimated the end date of seed production from parallel, non-destructive experiments involving sulfate-addition to wild rice mesocosms. The final date of seed collection was consistently close to day 260 for several years and experiments (Table S1). Using day 260 as the final date of seed production, we estimated a 20 % decrease in the true duration of seed production in amended plants compared to the unamended plants.

3.2. Seed production and vegetative biomass

Sulfate amended plants produced 33 % fewer seeds ($p = 0.03$), 50 % less total seedhead mass ($p = 0.01$), and 40 % total seedhead nitrogen ($p = 0.02$) compared to unamended plants (Table 2). Individual seeds were smaller by 33 % ($p = 0.02$), but individual seed N mass did not differ significantly between treatments. Sulfate amended plants had lower vegetative biomass (leaves and stems) during late flowering ($p < 0.01$, $n = 4$), but not prior life stages (Fig. S1). The experimental duration of seed production, calculated from the difference between

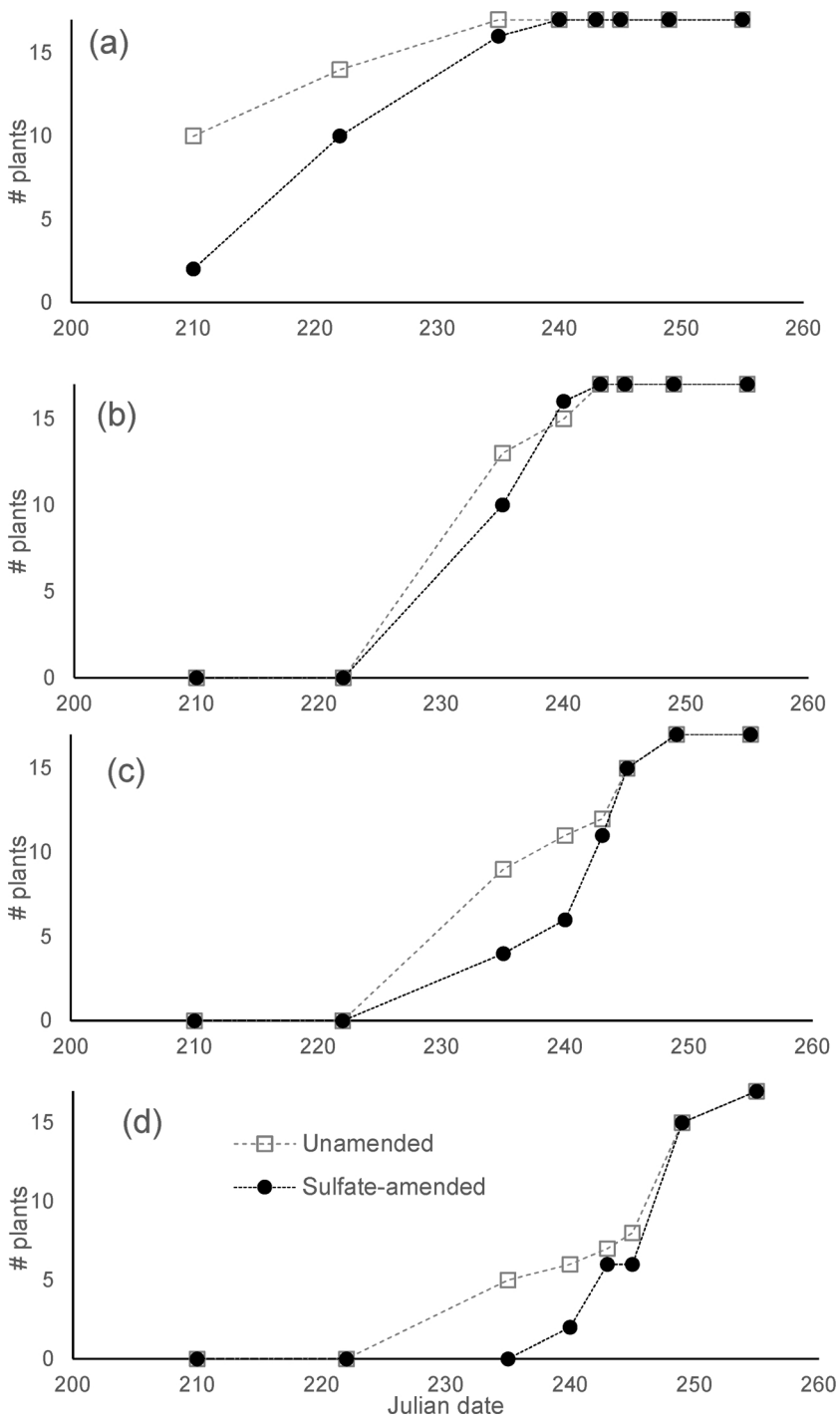

Fig. 1. Cumulative frequency of sulfate-amended (300 mg L^{-1}, filled circles) and unamended plants (open squares) that have initiated a) jointing, life stage 5, when internodes elongate just prior to reproduction, b) boot, life stage 6, when panicles emerge, c) mid flowering, life stage 8, when most flowers bloom, and d) seed production, life stage 10, when seed filling occurs.

first day seeds were observed and the day the plant was destructively sampled, was positively correlated with more filled seeds (p = 0.027), greater seed mass (p = 0.042), and more seed nitrogen (p = 0.012, Fig. 2).

3.3. Root geochemistry

Concentrations of AVS on amended root surfaces were one to two orders of magnitude higher than on unamended root surfaces during jointing, boot, mid flowering, and seed production (Table 2, Fig. S2). Porewater sulfate decreased from mid flowering until senescence, indicating that sulfate-amended plants were likely exposed to sulfide as a consequence of sulfate reduction (Fig. S3). On amended roots, AVS increased from about 10 μmol g^{-1} to about 65 μmol g^{-1} between jointing and boot. Concentrations of root surface sulfide then remained around 65 μmol g^{-1} until seed production. The AVS concentration doubled during seed production (life stages 10–11). On unamended roots, the concentration of sulfide steadily increased from 0.5 to 5 μmol g^{-1}, with the highest concentrations occurring during seed production. However, roots were not visibly black on unamended plants. Decreases

Table 2
Comparisons of acid volatile sulfide (AVS) concentration on root surfaces (μg g^{-1}) and of seed measurements in sulfate-amended (300 mg L^{-1}) and unamended conditions using a two-sample *t* test. AVS concentrations are compared during four reproductive life stages. The average for each treatment is reported with the standard deviation in parentheses (n = 4 for AVS during jointing, boot, and flowering; n = 12 for AVS during seed production, n = 10-12 for seed measurements; not all replicate plants had seeds).

Reproductive life stage	Sulfate-amended	Unamended	P value
Jointing	9.7 *(± 3.7)*	0.6 *(± 0.3)*	***P* < 0.01**
Boot	64.9 *(± 39.7)*	1.4 *(± 0.2)*	***P* = 0.05**
Mid flowering	68.9 *(± 42.9)*	2.6 *(± 0.5)*	***P* = 0.03**
Seed production	144.8 *(± 61.6)*	3.3 *(± 0.8)*	***P* < 0.01**
Seed Measurements			
Filled seed count (# per plant)	10.5 *(± 7.3)*	16 *(± 7.1)*	***P* = 0.03**
Total seedhead mass (g)	0.14 *(± 0.07)*	0.28 *(± 0.16)*	***P* = 0.01**
Total seedhead N mass (mg)	3.05 *(± 1.36)*	4.93 *(± 2.28)*	***P* = 0.02**
Individual seed mass (mg)	11.1 *(± 3.27)*	15.26 *(± 4.75)*	***P* = 0.02**
Individual seed N mass (mg)	0.26 *(± 0.15)*	0.28 *(± 0.08)*	*P* = 0.38
Seed N %	2.28 (± 0.63)	1.89 (± 0.48)	*P* = 0.06

in effective redox potential (E_h*), calculated from the ratio of Fe(III) to Fe(II) at root surfaces (Fig. 3, Fig. S4), occurred near both amended and unamended root surfaces between boot and jointing (life stage 5–6) and at the end of flowering (life stage 8–9). During seed production, the effective redox potential decreased more steeply at amended root surfaces.

4. Discussion

The phenology of seed production was delayed in sulfate-amended plants, suggesting ontogenetic drift induced by sulfide. Across both amended and unamended conditions, seedhead mass, seed number, and seedhead N mass correlated with length in the seed production life stage. In the presence of sulfate, delayed seed production and lower seed N uptake both co-occurred with a precipitous drop in redox potential and rapid accumulation of sulfide on roots.

In a natural setting, plants with a delayed start to seed production would have to compensate by either increasing N uptake rate or delaying senescence until a later calendar date. In our experiment, sulfate-amended plants contained less seedhead nitrogen than unamended plants, so the N uptake rate likely did not increase much, if at all. Our experimental design, requiring destructive sampling during seed production, was unable to test the completion of the seed production life stage. To address these limitations, we examined average end dates of seed production in parallel wild rice experiments. The date of last seed collection happened at similar dates or even earlier dates for sulfate-amended plants in these other experiments (Table S1). Thus, it seems likely that sulfate-amended plants do not extend the seed production life stage to compensate for a delay in the initiation of seed production and have a shorter true duration of seed production. Because the seed production yield (number of filled seeds, seedhead mass, seedhead nitrogen) is positively and linearly correlated with experimental duration of seed production (Fig. 2), we suggest that the implications of delayed initiation without delayed completion of seed production are lower reproductive outputs by plants.

The curious timing of iron sulfide precipitation on root surfaces coincident with the beginning of seed production suggests that plants

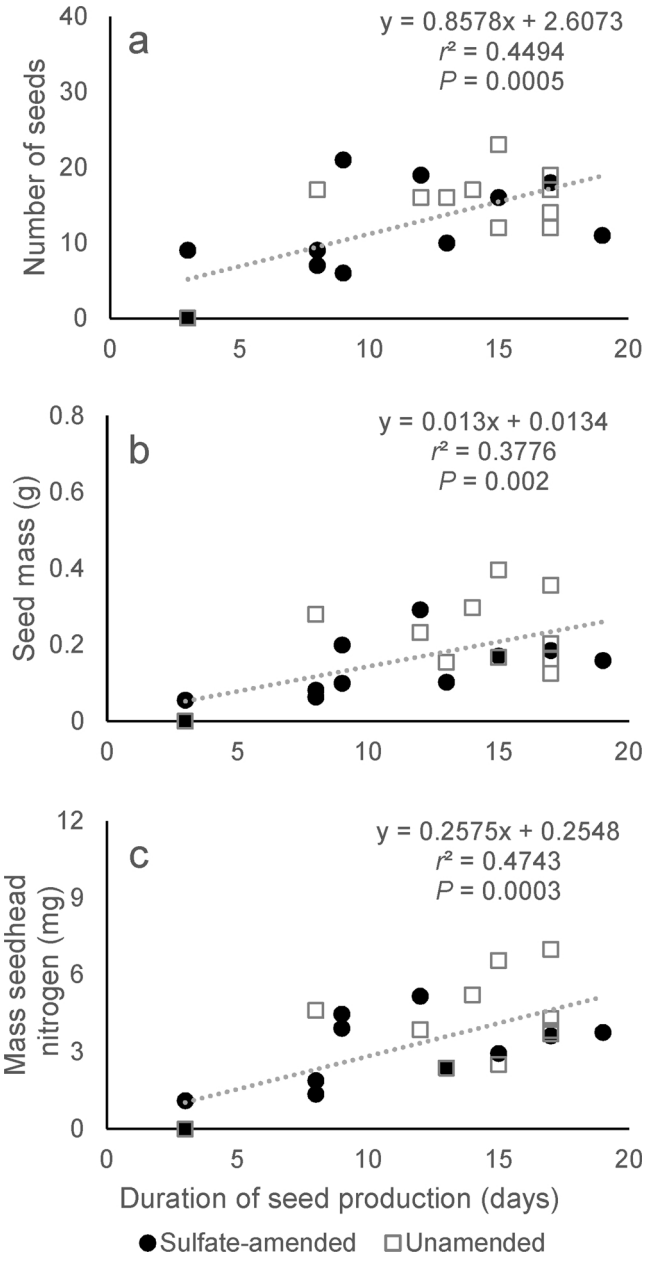

Fig. 2. Relationship between the experimental duration of seed production (days) and a) filled seed count, b) seedhead mass (g), and c) seedhead nitrogen (mg). Filled circles indicate sulfate-amended plants (300 mg L^{-1}) and open squares indicate unamended plants. End dates of duration for each plant were determined either by the date they entered seed maturity or by harvest date if they were harvested before reaching seed maturity.

influence the geochemistry of the sediments and that this influence changes during the plant's life cycle. The redox potential at the root surface, calculated from the ratio of Fe(III):Fe(II), decreased from jointing to boot (life stage 5–6), and again at the end of flowering (life stage 8–9). AVS concentrations increased on amended roots at the same life stages that redox declined. During seed production, the redox potential of amended and unamended plants diverged as the redox potential declined precipitously in amended plants. These decreases in redox potential reflect a net flow of electrons toward the plant root surfaces, suggesting a loss in the oxidizing capacity of the root surface. Transitions into new reproductive life stages are plausible times for plants to reallocate resources from photosynthetic tissues to reproductive tissues (Grava and Raisanen, 1978; McConnaughay and

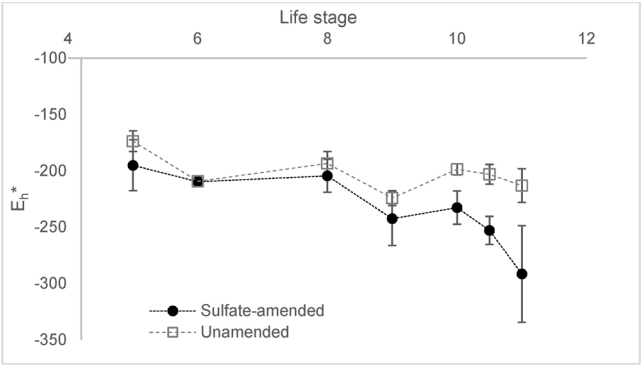

Fig. 3. Effective redox potential calculated from Fe(III) and Fe(II) concentration on roots amended with sulfate (300 mg L^{-1}, filled circles) or left unamended (open squares). Error bars show one standard deviation (n = 4). Life stages were assigned as 10, 10.5, and 11 for Julian dates 252, 257, and 264 respectively to show chronological progression in E_h* during seed production and maturity.

Coleman, 1999; Sims et al., 2012). Experiments with white rice (*Oryza sativa*), a closely related plant, have shown changes from iron oxide to iron sulfide in rhizosphere sediment as the plant entered flowering (Schmidt et al., 2011). We suggest that the change in redox conditions of the root surface at reproductive life stage transitions could be explained by a decrease in radial oxygen loss tied to the life stage of the plant, creating conditions conducive to iron sulfide formation in environments with elevated sulfur.

Plants concomitantly control and are controlled by sulfide. During vegetative growth life stages, plants maintain low sulfide in the rooting zone by releasing O_2 and accumulating Fe(III). However, at key reproductive life stage transitions, excess sulfide appears to overwhelm the plant's ability to oxidize the rhizosphere. The geochemical consequences of both life stage transition and excess sulfide are a precipitous drop in Fe(III):Fe(II) ratio and an accumulation of solid-phase sulfur on roots. The ecological consequences of life stage transitions in the presence of excess sulfide are a delay in reproductive phenology and a decrease in N uptake to seeds. Slower development rates in the presence of sulfide may delay life stage transitions and the geochemical consequences of these life stage transitions for redox potential. Our experimental design was not able to directly determine if redox potential decreased at a later date due to delayed phenology in amended plants. However, our observations do provide evidence that the net effect of sulfide-induced ontogenetic drift is shortened and decreased seed production. This finding hints at a phenological mechanism underlying sulfide-induced inhibition of nitrogen uptake observed in prior work (LaFond-Hudson et al., 2018). Considering that seedlings also experience high mortality when exposed to sulfide, 50 % less total seed mass in the presence of elevated sulfide may lead to rapid population declines, as has been previously observed in a mesocosm experiment (Pastor et al., 2017). Additionally, decreased density of plants in subsequent generations may lead to lower oxygen fluxes into sediment and exacerbate redox conditions that favor production of sulfide.

Sulfide inhibition of nutrient uptake has been demonstrated in other plants (Koch et al., 1990; Martin and Maricle, 2015), as has ontogenetic drift ((McConnaughay and Coleman, 1999; Sims et al., 2012), so other freshwater annual aquatic plant populations may face similar reproductive challenges if exposed to sulfide. Additionally, sulfide and iron interact with nutrients besides nitrogen. Iron plaques can adsorb phosphorus and metals, controlling their availability for uptake (St-Cyr and Campbell, 1996; Christensen and Sand-Jensen, 1998). Reduction of iron plaques in the presence of sulfide may affect uptake of both macro- and micronutrients. Some studies have investigated changes in radial oxygen loss over the growing season in perennial aquatic plants (Soana and Bartoli, 2013, 2014). However, because perennial plants may have different life cycle patterns of radial oxygen loss, the ways sulfide might interact with phenology or reproduction of perennial aquatic plants remains unknown. Clarifying how sulfide interacts with nutrients in rhizospheres of both annual and perennial plants may be important for understanding how wetlands or vegetated littoral zones respond to elevated sulfide conditions on an ecosystem level.

Redox conditions at root surfaces are closely tied to wild rice phenology. Sulfide, through delaying phenology, has the potential to control the timing of changes in redox conditions. By changing the timing and duration of reproductive life stages, sulfide's effects on phenology likely play a role in decreased survival of wild rice populations.

CRediT authorship contribution statement

Sophia LaFond-Hudson: Conceptualization, Methodology, Investigation, Data curation, Formal analysis, Writing - original draft, Visualization. **Nathan W. Johnson:** Conceptualization, Supervision, Writing - review & editing, Funding acquisition. **John Pastor:** Conceptualization, Supervision, Writing - review & editing, Funding acquisition. **Brad Dewey:** Conceptualization, Methodology, Investigation, Data curation, Writing - review & editing.

Declaration of Competing Interest

The authors declare that they have no conflict of interest.

Acknowledgements

This work was prepared by S. LaFond-Hudson, N. Johnson, J. Pastor, and B. Dewey using federal funds under award NA15OAR4170080 from Minnesota Sea Grant, National Sea Grant College Program, National Oceanic and Atmospheric Administration, U.S. Department of Commerce. The statements, findings, conclusions, and recommendations are those of the author(s) and do not necessarily reflect the views of NOAA, the Sea Grant College Program, or the U.S. Department of Commerce. Thank you to the Fond du Lac Band of Lake Superior Chippewa for providing sediment.

Appendix A. Supplementary data

Supplementary material related to this article can be found, in the online version, at doi:https://doi.org/10.1016/j.aquabot.2020.103230.

References

Allam, A.I., Hollis, J.P., 1972. Sulfide inhibition of oxidases in rice roots. Phytopathology 62, 634–639.
Armstrong, W., 1980. Aeration in higher plants. In: Woolhouse, H.W. (Ed.), Advances in Botanical Research. Academic Press, pp. 225–332.
Armstrong, J., Armstrong, W., Beckett, P.M., 1992. Phragmites australis: venturi- and humidity-induced pressure flows enhance rhizome aeration and rhizosphere oxidation. New Phytol. 120, 197–207. https://doi.org/10.1111/j.1469-8137.1992.tb05655.x.
Brouwer, H., Murphy, T.P., 1994. Diffusion method for the determination of acid-volatile sulfides (AVS) in sediment. Environ. Toxicol. Chem. 13, 1273–1275. https://doi.org/10.1002/etc.5620130808.
Carlson, J., Yarbro, L.A., Barber, T.R., 1994. Relationship of sediment sulfide to mortality of Thalassia testudinum in Florida Bay. Bull. Mar. Sci. 54, 733–746.
Christensen, K.K., Sand-Jensen, K., 1998. Precipitated iron and manganese plaques restrict root uptake of phosphorus in Lobelia dortmanna. Can. J. Bot. 76, 2158–2163. https://doi.org/10.1139/b98-181.
Coleman, J.S., McConnaughy, K.D.M., Ackerly, D.D., 1994. Interpreting phenotypic variation in plants. Tree 9, 187–191.
Colmer, T.D., 2003. Aerenchyma and an inducible barrier to radial oxygen loss facilitate root aeration in upland, Paddy and deep-water rice (Oryza sativa L.). Ann. Bot. 91, 301–309. https://doi.org/10.1093/aob/mcf114.
Dacey, J.W.H., 1980. Internal winds in water lilies: an adaptation for life in anaerobic sediments. Science 210, 1017–1019.
Fond du Lac Band of Lake Superior Chippewa, 2018. Expanding the narrative of tribal health: the effects of wild rice water quality rule changes on tribal health. Health Impact Assess. 68.
Grava, J., Raisanen, K.A., 1978. Growth and nutrient accumulation and distribution in

wild rice 1. Agron. J. 70, 1077–1081. https://doi.org/10.2134/agronj1978.00021962007000060044x.
Jorgenson, K.D., Lee, P.F., Kanavillil, N., 2012. Ecological relationships of wild rice, Zizania spp. 11. Electron microscopy study of iron plaques on the roots of northern wild rice (Zizania palustris). Botany 91, 189–201. https://doi.org/10.1139/cjb-2012-0198.
Koch, M.S., Mendelssohn, I.A., 1989. Sulphide as a soil phytotoxin: differential responses in two marsh species. J. Ecol. 77, 565–578. https://doi.org/10.2307/2260770.
Koch, M.S., Mendelssohn, I.A., McKee, K.L., 1990. Mechanism for the hydrogen sulfide-induced growth limitation in wetland macrophytes. Limnol. Oceanogr. 35, 399–408. https://doi.org/10.4319/lo.1990.35.2.0399.
LaFond-Hudson, S., Johnson, N.W., Pastor, J., Dewey, B., 2018. Iron sulfide formation on root surfaces controlled by the life cycle of wild rice (Zizania palustris). Biogeochemistry 141, 95–106. https://doi.org/10.1007/s10533-018-0491-5.
Lamers, L.P.M., Tomassen, H.B.M., Roelofs, J.G.M., 1998. Sulfate-induced eutrophication and phytotoxicity in freshwater wetlands. Environ. Sci. Technol. 32, 199–205. https://doi.org/10.1021/es970362f.
Martin, N.M., Maricle, B.R., 2015. Species-specific enzymatic tolerance of sulfide toxicity in plant roots. Plant Physiol. Biochem. 88, 36–41. https://doi.org/10.1016/j.plaphy.2015.01.007.
Marzocchi, U., Benelli, S., Larsen, M., et al., 2019. Spatial heterogeneity and short-term oxygen dynamics in the rhizosphere of Vallisneria spiralis: implications for nutrient cycling. Freshw. Biol. 64, 532–543. https://doi.org/10.1111/fwb.13240.
McConnaughay, K.D.M., Coleman, J.S., 1999. Biomass allocation in plants: ontogeny or optimality? A test along three resource gradients. Ecology 80, 2581–2593. https://doi.org/10.1890/0012-9658(1999)080[2581:BAIPOO]2.0.CO;2.
Mendelssohn, I.A., Kleiss, B.A., Wakeley, J.S., 1995. Factors controlling the formation of oxidized root channels: a review. Wetlands 15, 37–46. https://doi.org/10.1007/BF03160678.
Pastor, J., Dewey, B., Johnson, N.W., et al., 2017. Effects of sulfate and sulfide on the life cycle of Zizania palustris in hydroponic and mesocosm experiments. Ecol. Appl. 27, 321–336. https://doi.org/10.1002/eap.1452.
Schmidt, H., Eickhorst, T., Tippkötter, R., 2011. Monitoring of root growth and redox conditions in paddy soil rhizotrons by redox electrodes and image analysis. Plant Soil 341, 221–232. https://doi.org/10.1007/s11104-010-0637-2.
Sims, L., Pastor, J., Lee, T., Dewey, B., 2012. Nitrogen, phosphorus and light effects on growth and allocation of biomass and nutrients in wild rice. Oecologia 170, 65–76. https://doi.org/10.1007/s00442-012-2296-x.
Soana, E., Bartoli, M., 2013. Seasonal variation of radial oxygen loss in Vallisneria spiralis L.: an adaptive response to sediment redox? Aquat. Bot. 104, 228–232. https://doi.org/10.1016/j.aquabot.2012.07.007.
Soana, E., Bartoli, M., 2014. Seasonal regulation of nitrification in a rooted macrophyte (Vallisneria spiralis L.) meadow under eutrophic conditions. Aquat. Microb. Ecol. 48, 11–21. https://doi.org/10.1007/s10452-013-9462-z.
St-Cyr, L., Campbell, P.G.C., 1996. Metals (Fe, Mn, Zn) in the root plaque of submerged aquatic plants collected in situ: relations with metal concentrations in the adjacent sediments and in the root tissue. Biogeochemistry 33, 45–76.
Stover, E.L., 1928. The roots of wild rice Zizania Aquatica L. Ohio J. Sci. 28 (7).
Stumm, W., Morgan, J.J., 2012. Aquatic Chemistry: Chemical Equilibria and Rates in Natural Waters Vol. 126 John Wiley & Sons.
Trolldenier, G., 1988. Visualisation of oxidizing power of rice roots and of possible participation of bacteria in iron deposition. Zeitschrift für Pflanzenernährung und Bodenkunde 151, 117–121. https://doi.org/10.1002/jpln.19881510209.
Van der Welle, M.E.W., Niggebrugge, K., Lamers, L.P.M., Roelofs, J.G.M., 2007. Differential responses of the freshwater wetland species Juncus effusus L. and Caltha palustris L. to iron supply in sulfidic environments. Environ. Pollut. 147, 222–230. https://doi.org/10.1016/j.envpol.2006.08.024.

JGR Biogeosciences

RESEARCH ARTICLE
10.1029/2022JG006809

Sulfur Geochemistry Destabilizes Population Oscillations of Wild Rice (*Zizania palustris*)

Sophia LaFond-Hudson[1,2], Nathan W. Johnson[1], John Pastor[3], and Brad Dewey[3]

[1]Department of Civil Engineering, University of MN Duluth, Duluth, MN, USA, [2]Now at Oak Ridge National Laboratory, Oak Ridge, TN, USA, [3]Department of Biology, University of Minnesota Duluth, Duluth, MN, USA

Key Points:

- Populations exposed to elevated sulfate went extinct in 6 years, overriding interannual biomass oscillations
- Iron addition and litter removal slightly alleviated sulfide toxicity but did not prevent population extinction
- Stability of oscillating populations can be evaluated with only a few years' data using an eigenvalue

Correspondence to:

S. LaFond-Hudson,
lafo0062@d.umn.edu

Citation:

LaFond-Hudson, S., Johnson, N. W., Pastor, J., & Dewey, B. (2022). Sulfur geochemistry destabilizes population oscillations of wild rice (*Zizania palustris*). *Journal of Geophysical Research: Biogeosciences*, *127*, e2022JG006809. https://doi.org/10.1029/2022JG006809

Received 19 JAN 2022
Accepted 30 JUN 2022

Author Contributions:

Conceptualization: Nathan W. Johnson, John Pastor
Funding acquisition: Nathan W. Johnson, John Pastor
Investigation: Sophia LaFond-Hudson, Nathan W. Johnson, John Pastor, Brad Dewey
Methodology: Sophia LaFond-Hudson, Nathan W. Johnson, John Pastor, Brad Dewey
Writing – original draft: Sophia LaFond-Hudson
Writing – review & editing: Sophia LaFond-Hudson, Nathan W. Johnson, John Pastor, Brad Dewey

Abstract Elevated inputs of sulfate to freshwater systems can increase sulfide concentrations in anoxic soils and subsequently destabilize aquatic plant populations, but the interactions between sulfate, other geochemical cycles, and interannual plant population cycles are poorly understood. Increased sulfate loading increases mineralization of nitrogen from litter, but the sulfide produced during this process can limit nitrogen uptake by plants. In some cases, iron may mitigate sulfide's impacts on plants by precipitating iron sulfide. We examined the interannual effects of sulfate loading on mesocosm populations of wild rice, an emergent aquatic plant that undergoes population oscillations and is sensitive to sulfide. Using experimental mesocosms with self-perpetuating populations, we investigated how population dynamics respond to manipulations of surface water sulfate (10 mg L^{-1} or 300 mg L^{-1}), sediment iron (4.3 mg g^{-1} or 10.9 mg g^{-1} dry weight), and shoot litter (present or removed). Populations exposed to constant 10 mg L^{-1} sulfate concentrations had stable biomass oscillations of approximately 3-year periods, consistent with previous studies that demonstrated litter-driven oscillations in nitrogen availability. Populations exposed to 300 mg L^{-1} sulfate concentrations produced fewer and smaller seeds and declined to extinction in 6 years or less. We did not find a strong effect of iron loading or litter removal on wild rice biomass or seed production. Our observations show the potential of elevated surface water sulfate to rapidly destabilize wild rice populations under varying iron and organic carbon concentrations.

Plain Language Summary Plants that naturally grow in freshwater do not survive well if the water contains elevated concentrations of sulfate. Sulfate reduction produces sulfide that subsequently inhibits the uptake of nitrogen, an essential plant nutrient. Some annual plants go through boom-bust cycles with years alternating between high and low biomass because nitrogen takes more than a year to be released from dead plant matter. We investigated the combined effect of sulfate and natural biomass cycles on the stability of wild rice populations by growing plants in large tanks and exposing them to high-sulfate and low-sulfate concentrations, high and low iron concentrations, and with plant matter from the previous growing season either returned or removed. Nearly all plant populations exposed to high sulfate had died by 6 years into the experiment, regardless of iron concentration or litter removal. We show a method to analyze population stability with just a few years of data.

1. Introduction

Northern wild rice (*Zizania palustris*) is one of four species in the genus *Zizania*, which are the only native aquatic grains in North America. The range of northern wild rice (hereafter wild rice) is centered across the Great Lakes region and is most abundant in the rivers and lakes of the watersheds of Lakes Superior and Michigan in northern Minnesota, Wisconsin, and Ontario. Wild rice beds are usually very large (tens or hundreds of hectares) and monotypic. Because of its widespread distribution and tendency to form large monotypic stands, wild rice has great potential to control the quality of waters draining into Lakes Superior and Michigan and influence the food supply for waterfowl, muskrats, and other members of the food web. In addition, harvesting and eating wild rice are essential traditional practices that provide food sovereignty and well-being for the native Ojibway people of the watersheds of Lakes Superior and Michigan (Fond du Lac Band of Lake Superior Chippewa, 2018). Therefore, the productivity, perpetuation, and restoration of wild rice are of great ecological and cultural significance.

Production of wild rice biomass is limited by the supply of nitrogen from decomposing plant litter, sediment organic matter, and hydrologic inputs (Pastor & Walker, 2006; Sims et al., 2012; Walker et al., 2006, 2010). Because it is an annual plant, wild rice's nitrogen requirements must be fully supported by uptake during each year. Over 60% of nitrogen uptake happens during a 2-week window in early summer (Grava & Raisanen, 1978;

Sims et al., 2012). Nitrogen, however, is not released from the previous year's litter until later in summer or even the following year (Hildebrandt et al., 2012; Sain, 1984; Walker et al., 2010). In fact, there is considerable microbial immobilization of nitrogen into fresh litter during the period when the demands of wild rice growth for nitrogen are greatest (Hildebrandt et al., 2012; Walker et al., 2010). The coincidence of microbial nitrogen immobilization with the period of rapid nitrogen uptake causes wild rice biomass and litter production to cycle with a period of approximately 4 years (Pastor & Walker, 2006; Walker et al., 2010).

Inputs of sulfate from bedrock weathering, mine drainage, and agriculture enhance sulfide production in natural wild rice ecosystems (Bailey et al., 2017; Lamers et al., 2013; Myrbo et al., 2017a). Wild rice production appears to be adversely impacted by sulfide in the vicinity of its rooting zone. The survival of juvenile seedlings and weights of seeds decrease with increased hydrogen sulfide concentrations in wild rice's rooting zone in aquatic sediments (Pastor et al., 2017). The production of sulfide may be coupled to increased litter deposited in sediment during productive years of the wild rice population cycle. These large litter cohorts could reduce sediment redox potential (Eh) by providing additional labile carbon to support additional bacterial growth and hence oxygen demand the following year, thereby enhancing the potential for reduction of sulfate to sulfide (Azam et al., 1991; Gao et al., 2003, 2004).

Other biogeochemical reactions in the sediments may impede the bioavailability of sulfide to wild rice roots. The most important reaction is precipitation of sulfide with reduced iron (Morse et al., 1987). In both mesocosm and lake studies (Bailey et al., 2017; Myrbo et al., 2017a), iron in sediments appear to exert a strong control on the accumulation of dissolved sulfide in sediments. Bulk sediment iron content is strongly associated with lower porewater sulfide in field conditions and mitigates sulfide toxicity to macrophytes in other aquatic ecosystems (Lamers et al., 2002; Ruiz-Halpern et al., 2008; Van der Welle et al., 2007).

However, iron sulfide can precipitate on roots of mature plants and is associated with impaired nitrogen uptake and inhibited seed production (LaFond-Hudson et al., 2018, 2020a). Plant-mediated gas transport of oxygen from the atmosphere into the rhizosphere allows formation of iron oxides on root surfaces, and oxygen fluxes are typically highest when plants are photosynthetically active (Blossfeld et al., 2011; Han et al., 2018; Marzocchi et al., 2019). As observed on many emergent macrophytes, iron oxide forms on wild rice roots as the plant grows (Jorgenson et al., 2012; Mendelssohn et al., 1995; Sundby et al., 1998). At maturity and the start of seed production, however, root plaques transition from iron oxide to iron sulfide if porewater sulfate is abundant (LaFond-Hudson et al., 2018). We have imaged iron sulfide plaques and quantified plaque iron and sulfide concentrations from plants grown in mesocosms with 300 mg L^{-1} sulfate (Pastor et al., 2017) and have visually observed black root plaques in the field at lower sulfate concentrations (unpublished data). Plants that accumulate greater concentrations of iron sulfide plaques have lower seed nitrogen mass (LaFond-Hudson et al., 2018, 2020a).

There are, therefore, complex and as yet poorly understood couplings among biomass and litter cycles, nitrogen availability, sulfide inhibition of seed production, control of sulfide concentrations in sediments by iron and litter, and precipitation of iron sulfide on roots during seed production. Here, we investigate how litter-driven population oscillations interact with sulfate geochemistry in wild rice using controlled mesocosm experiments that allow us to scale rhizosphere geochemistry-plant physiology interactions from individual plants to an entire population for several generations. In our mesocosms, we elevated geochemical inputs of sulfate and iron and manipulated carbon through the presence or absence of litter. We investigated: (a) the patterns of biomass oscillations in high-sulfate and low-sulfate conditions, and (b) whether litter and iron enhance or alleviate sulfate's effects on biomass oscillations through the production and precipitation of sulfide.

2. Methods

2.1. Experimental Design

The interactions of sulfate, iron, and litter in wild rice sediment and their effect on wild rice population dynamics were studied using 40 mesocosms. Polyethylene stock tanks (High Country Plastics 400 L, 132 × 78 × 61 cm) were used to assemble the mesocosms (Figure 1). Sediment in the tanks was taken from Rice Portage Lake (MN Lake ID 09003700, 46.7038, −92.6829) on the Fond du Lac Band of Lake Superior Ojibway Reservation in Carlton County, Minnesota (Table 1). This lake is a productive wild rice lake with little surrounding development and its sediment has been used successfully to grow wild rice in previous experiments (Pastor et al., 2017). Sediment was homogenized before it was added to the tanks. Clean sand (10 cm) was added to the bottom of the

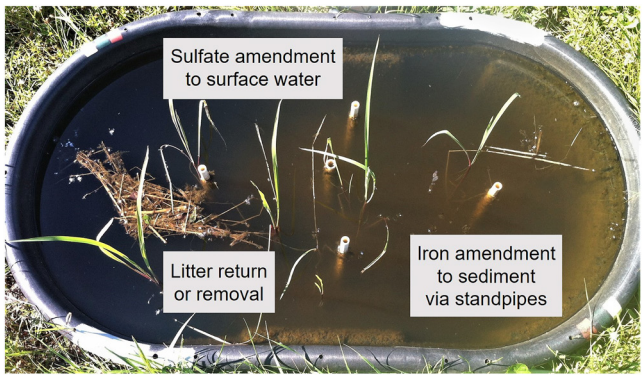

Figure 1. Picture of a mesocom showing the application of sulfate, iron, and litter treatments. The center standpipe was used to moderate the water level after rain events. The other four standpipes connect to a ring of perforated PVC pipes in the sediment to allow release of iron(II) chloride. Sulfate was applied as sodium sulfate several times over each growing season to maintain surface water concentrations near 300 mg L^{-1} sulfate. Litter was weighed at the end of each growing season, and either returned to the mesocosms, or permanently removed.

tanks before 50 L of lake sediment were placed in each tank, resulting in a sediment depth of about 10 cm on top of 10 cm of sand. Water levels were maintained at 22 cm with a drain standpipe during precipitation and well water additions to account for evaporation. These depths of sand, sediment, and water represent typical wild rice rooting depth and water column heights in the field and have been used in several wild rice mesocosm experiments previously (Hildebrandt et al., 2012; Pastor et al., 2017; Walker et al., 2010).

To test the effects and interactions of sulfate, iron, and litter, we used a factorial design with five replicates for each of eight combinations of elevated or background sulfate, elevated or background iron, and the presence or absence of litter (Figure 1). These combinations were randomly assigned to the tanks in the first year of the experiment. For high-sulfate treatments, enough sodium sulfate was added to the surface water to bring the sulfate concentration to a target level of 300 mg L^{-1}. Surface water sulfate concentrations were tested weekly and sodium sulfate was added as required to maintain concentrations at the target level of 300 mg L^{-1} throughout the growing season for the duration of the experiment. The low-sulfate tanks were filled with water from an on-site well with concentrations around 10 mg L^{-1} and received no additional sulfate additions except for precipitation, which averaged 2.3 ± 1.5 mg L^{-1} sulfate. The sulfate concentrations in the low-sulfate tanks averaged around 7 mg L^{-1} over several years (Pastor et al., 2017). The low-sulfate conditions for our experiment are still higher than the median sulfate concentration of Minnesota wild rice waters, 1.8 mg L^{-1} (Myrbo et al., 2017a), but is just below Minnesota's protective sulfate standard for wild rice waters. At 300 mg L^{-1}, our high-sulfate treatment is close to the EPA's secondary standard for sulfate in drinking water (250 mg L^{-1}) and represents surface water concentrations of a few lakes and rivers in Minnesota that contain wild rice (Myrbo et al., 2017a). Prior to both sulfate and iron amendment, sediment iron was extracted from homogenized sediment samples using 1 M HCl and quantified on a Varian fast sequential flame atomic absorption spectrometer with an acetylene torch (Federation & Association, 2005). The sediment initially contained 77 µmol Fe g^{-1} dry weight (Table 1), 85% of which was Fe(II) (Phenanthroline method, see Section 2.2). Each iron-amended tank received 96 g Fe^{2+}, bringing total iron concentrations up to approximately 196 µmol Fe g^{-1}, or 10.9 mg g^{-1} dry weight. This amendment level aimed to noticeably increase iron concentrations without causing iron toxicity (Kinsman-Costello et al., 2015). Iron was applied gradually in four separate aliquots during the first growing season. For each addition, 75 g $FeCl \cdot 4H_2O$ was dissolved in 400 mL well water and added directly into the sediment through PVC standpipes connected to a buried perforated PVC ring. The standpipes and ring were flushed with 100 mL of tank water immediately after the iron(II) chloride was injected. Samples of pore water iron were taken several times over the course of the first growing season in 10 points distributed across the tank to ensure that the iron loading was distributed evenly. Noniron tanks did not receive additional iron except for occasional well water that contained 0.17 mg L^{-1} Fe. Noniron tanks did not have a buried PVC ring, but all mesocosms had a center standpipe draining into an external bucket to restore the water level after rain events.

Table 1
Initial Bulk Sediment Physical and Chemical Characteristics

Sediment property	Value
Porosity	0.87
Bulk density	0.29 g cm^{-3}
Percent solids	30
Solid-phase acid volatile sulfide (AVS)	0.346 ± 0.054 µmol g^{-1}
Solid-phase extractable iron	76.7 ± 5.1 µmol g^{-1}
Solid-phase ferrous iron	65.2 ± 4.8 µmol g^{-1}
Porewater sulfide	0.659 ± 0.239 µmol L^{-1}
Porewater ferrous iron	435 ± 200 µmol L^{-1}
Initial solid phase S:Fe ratio	0.00450
Initial porewater ΣS^{2-}:Fe^{2+} ratio	0.0015

Note. Sulfide was measured from initial sediment and porewater iron is an average from fall measurements in tanks unamended with iron.

To test the effect of shoot litter cohorts on sulfide production, shoot litter produced by the wild rice population was retained in half the tanks and removed from the remaining tanks. Litter removal was chosen as the experimental treatment rather than litter addition because in typical freshwater, organic-rich wild rice habitats, sulfide production is generally limited by sulfate rather than organic carbon, so increasing litter may have had little effect. Only aboveground litter was removed for two reasons: (a) to minimize sediment disturbance, and (b) to focus on litter effects on sulfide production. Litter-driven biomass oscillations are driven primarily by recalcitrant root litter (Walker et al., 2010), so aboveground litter manipulation was not

expected to disrupt interannual cycles. Initial organic carbon content of the sediment was 14.8 ± 1.7% by dry weight (Pastor et al., 2017).

2.2. Geochemical Sampling and Analysis

In 2019 (year 5 of study), passive diffusion samplers (peepers) were installed in the tanks during vegetative growth (July) and seed production (September) to obtain porewater measurements from discrete depths in the top six cm of sediment. The peepers were placed in deionized water that was bubbled with nitrogen for 1 week prior to installation (Johnson et al., 2019). The peepers were transported to mesocosms in degassed water and installed in three tanks for each treatment. Each peeper contained four wells, the top of which was in the flocculant litter layer at the sediment surface and the bottom of which was approximately six cm below the sediment surface. Two weeks after peepers were installed, each peeper was removed and quickly placed in a large, resealable plastic bag purged with nitrogen gas to keep porewater anoxic during porewater extraction. Approximately 6 mL of porewater from each well was extracted with a syringe and allocated for immediate sulfide and iron measurements in vials preloaded with reagents. A separate aliquot was used to measure pH within 30 s.

Iron(II) and sulfide were quantified colorimetrically using the phenanthroline and methylene blue methods, respectively, on a HACH DR5000 UV-Vis spectrophotometer (Federation & Association, 2005). The pH of the pore water was measured by placing a calibrated ThermoScientific Orion pH electrode in porewater immediately after it was extracted from peepers.

2.3. Biological Sampling and Analysis

Seedlings usually began to germinate around mid-May. When seedlings grew to the water surface, populations in each mesocosm were thinned to approximately 30 plants per tank, which is the optimal density to limit competition and minimize overlapping rhizospheres (Lee, 2002). In August, as plants began to flower, six plants from each tank were randomly selected and tagged. Seed data were collected from these six plants and extrapolated to the total number of plants in the tank. Seeds from the remaining plants were left in the tank to reseed the sediment for the next year. Seeds were sorted as filled or unfilled by visual inspection, counted, and dried at 65 °C and weighed to determine seed mass. After all plants had completely senesced in October, all aboveground biomass was removed and weighed with a small subsample dried at 65 °C and weighed for moisture correction. The litter that was not dried was returned to the mesocosms assigned to retain litter within a few days.

2.4. Data Analysis

The data collected in this experiment are available at the Digital Repository for University of Minnesota (LaFond-Hudson et al., 2020b). Porewater data collected from peepers were examined to understand how porewater sulfide to iron ratios and saturation with respect to FeS were changed 5 years after geochemical manipulation. A three-way ANOVA was used to test the effect of each geochemical manipulation (sulfate, iron, litter). Repeated measures ANOVAs were used to determine the effect of time, sulfate addition, iron addition, and litter removal on biological traits and porewater measurements. Data were checked for normality and heteroscedasticity using R's standard diagnostic plots and for sphericity using the ez R package (Lawrence, 2016), which provides sphericity corrections in the case of violated assumptions. For porewater data, nondetects (12% of samples) and lost samples (11%) were removed. Zeros were not removed in biological data, as these were true absences of plant or seed tissue. Including zeros in biological data resulted in large variance under high-sulfate conditions, making it harder to detect differences between treatments using ANOVA tests. However, averages calculated including zeros (extinction of the population) represent the effects of high sulfate more completely than removing zeros.

To test the propensity of the population to oscillate in high-sulfate and low-sulfate conditions, we regressed the change in vegetative biomass ($B(t) - B(t-1)$) against the vegetative biomass from the previous year ($B(t-1)$). A negative slope of this regression indicates that high productivity 1 year leads to lower productivity the following year and, conversely, that years with low productivity are followed by years with higher productivity (Walker et al., 2010). The slope of this line is $\partial(\mathrm{d}B/\mathrm{d}t)/\partial B$, which is effectively an eigenvalue of system. A critical value of -1 of this eigenvalue defines a Hopf bifurcation giving birth to stable limit cycles (Pastor & Walker, 2006; Strogatz, 1994; Walker et al., 2010). A slope of -1 or more negative indicates propensity for stable oscillations,

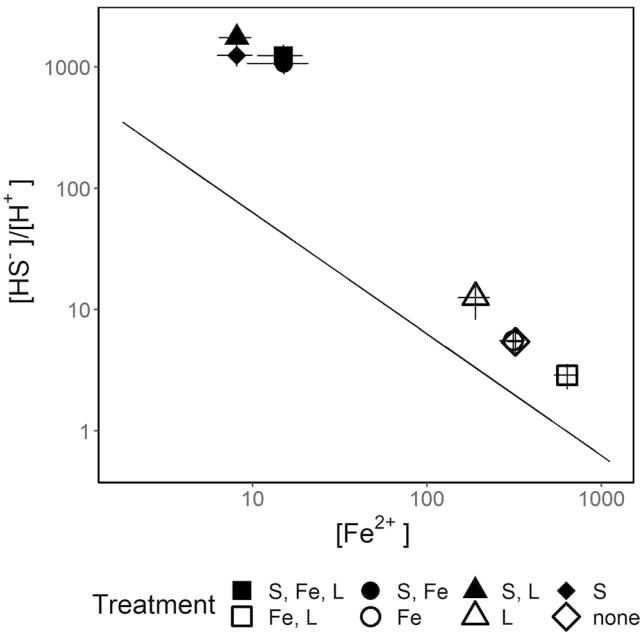

Figure 2. Comparison of ferrous iron (μmol L^{-1}) and sulfide concentrations (both sulfide and H+ in mol L^{-1}) in sediment porewater after 5 years of sulfate amendment (S), iron amendment (Fe), and litter retention (L). Data points represent average porewater measurements for each treatment (n = 12–30; most n = 24). Error bars represent the standard error around the mean. Porewater was collected 2, 4, and 6 cm below the sediment surface using peepers. Open symbols are for mesocosms with background sulfate concentrations and closed symbols are for mesocosms with nominal sulfate concentrations of 300 mg L^{-1} in overlying water. The line depicts the ion activity product at saturation for iron and bisulfide at pH 7.0 (log K_{sp} = −3.2). Porewater pH in elevated sulfate mesocosms ranged from 6.85 to 8.56 with a mean of 7.33 while porewater pH in low-sulfate mesocosms averaged ranged from 6.18 to 8.83 with a mean of 6.67.

while a slope between −1 and 0 indicates dampened oscillations (Walker et al., 2010). Dampened oscillations will eventually converge on a stable value of biomass, which may include zero (extinction). When no biomass is produced the following year, the population is at the boundary line $y = -x$ and the population is extinct. Vegetative biomass, rather than total biomass (vegetative + seeds), was used in this analysis because asynchrony in nitrogen mineralization and nitrogen uptake is expected to affect plants most during vegetative growth (Grava & Raisanen, 1978; Walker et al., 2010).

3. Results

3.1. Geochemical Context

Both high-sulfate and low-sulfate conditions contained sulfide and iron concentrations that favored precipitation of FeS (ion activity product > Ksp, Figure 2) in the fifth year of the study. Sulfate amendments to the surface water increased porewater sulfide and pH, and decreased porewater ferrous iron concentrations ($p < 0.001$ for all, Table 2). Sulfate addition raised porewater sulfide from an average of 4 μmol L^{-1} in unamended tanks to 110 μmol L^{-1} and lowered porewater ferrous iron concentrations by a similar order of magnitude, from 309 to 12 μmol L^{-1}. The pH in high-sulfate mesocosms was 0.65 units higher than in low-sulfate conditions (7.32, 6.67). Iron amendment increased porewater ferrous iron concentrations by approximately 70–80% ($p < 0.001$, Table 2) but did not notably change sulfide or pH. Litter removal did not significantly change sulfur or iron geochemistry.

3.2. Geochemical Effects on Biomass and Reproduction

All measured traits of wild rice growth and reproduction changed with time (Table 3). Sulfate addition strongly and consistently decreased all measured traits of wild rice growth (Table 3). The main effects of iron addition and litter removal were much weaker and inconsistent relative to sulfate addition, therefore we examined how iron and litter affected wild rice growth and reproduction using separate repeated measures ANOVAs for the high and low sulfur populations, respectively.

Total aboveground biomass density (hereafter referred to as biomass) was similar between high-sulfate and low-sulfate populations during the first year of the experiment (100 g m^{-2}), but biomass in high-sulfate populations declined to less than 5 g m^{-2} during the subsequent 5 years (Figure 3). In 2017, 4 years into the experiment, 8 out of the 20 populations receiving high sulfate loads produced no biomass regardless of iron addition and litter removal. Seven populations recovered partially in 2018, possibly from the germination of seeds from previous years buried in the sediment, but by 2019, 16 out of these 20 populations produced no biomass. In low-sulfate

Table 2
The Effect of Five Years of Sulfate, Iron, and Litter Additions on Porewater Concentrations of Sulfide and Iron, Porewater pH, and the Saturation Index With Respect to FeS Calculated From the Former Three Measurements in 2019 (Three-Way ANOVA)

Variable	Sulfate	Iron	Litter	Significant interactions
Porewater sulfide	**$p < 0.001$**	$p = 0.53$	$p = 0.64$	S × Fe, Litter × Fe, S × Litter × Fe
Porewater iron	**$p < 0.001$**	**$p < 0.001$**	$p = 0.16$	
Porewater pH	**$p < 0.001$**	$p = 0.64$	$p = 0.57$	S × Litter × Fe
Saturation index of FeS	**$p < 0.001$**	$p = 0.19$	$p = 0.96$	

Note. Significant interactions (in bold) refer to combinations of sulfate, iron, and/or litter that are significant at $p < 0.05$.

Table 3
Repeated Measures ANOVA Testing the Influence of Sulfate Amendment, Iron Amendment, and Litter Removal on Wild Rice Growth and Reproduction for 2014–2020

Trait	Year	Sulfate	Iron	Litter	Significant interactions
Vegetative biomass	$\mathbf{p < 0.001}$	$\mathbf{p < 0.001}$	$p = 0.81$	$p = 0.44$	S × L × Fe × Year, S × L × Year, S × Year, Fe × Year
Population seed mass	$\mathbf{p < 0.001}$	$\mathbf{p < 0.001}$	$p = 0.59$	$p = 0.09$	S × L × Year, S × Year
Filled seed ratio	$\mathbf{p < 0.001}$	$\mathbf{p < 0.001}$	$\mathbf{p < 0.001}$	$p = 0.25$	S × Year
Mass per filled seed	$\mathbf{p < 0.001}$	$\mathbf{p < 0.001}$	$\mathbf{p = 0.002}$	$p = 0.40$	S × Year, Fe × Year
Total biomass	$\mathbf{p < 0.001}$	$\mathbf{p < 0.001}$	$p = 0.71$	$p = 0.23$	S × Fe × L × Year, S × L × Year, S × Year
High-sulfate conditions					
Vegetative biomass	$\mathbf{p < 0.001}$	–	$p = 0.82$	$p = 0.83$	L × Year, Fe × L × Year, Fe × Year
Population seed mass	$\mathbf{p < 0.001}$	–	$p = 0.28$	$p = 0.67$	
Filled seed ratio	$\mathbf{p < 0.001}$	–	$\mathbf{p = 0.01}$	$p = 0.42$	
Mass per filled seed	$\mathbf{p < 0.001}$		$\mathbf{p = 0.04}$	$p = 0.20$	
Total biomass	$\mathbf{p < 0.001}$	–	$p = 0.74$	$p = 0.97$	L × Year, Fe × L × Year
Low-sulfate conditions					
Vegetative biomass	$\mathbf{p < 0.001}$	–	$p = 0.68$	$p = 0.30$	Fe × Year
Population seed mass	$\mathbf{p < 0.001}$	–	$p = 0.82$	$p = 0.08$	
Filled seed ratio	$\mathbf{p < 0.001}$	–	$\mathbf{p = 0.01}$	$p = 0.41$	Fe × Year
Mass per filled seed	$\mathbf{p < 0.001}$	–	$\mathbf{p = 0.02}$	$p = 0.86$	Fe × Year
Total biomass	$\mathbf{p < 0.001}$	--	$p = 0.82$	$p = 0.18$	

Note. Bold values highlight p-values < 0.05. Separate tests for high-sulfate and low-sulfate conditions are also included. Interactions are listed if significance is $p < 0.05$.

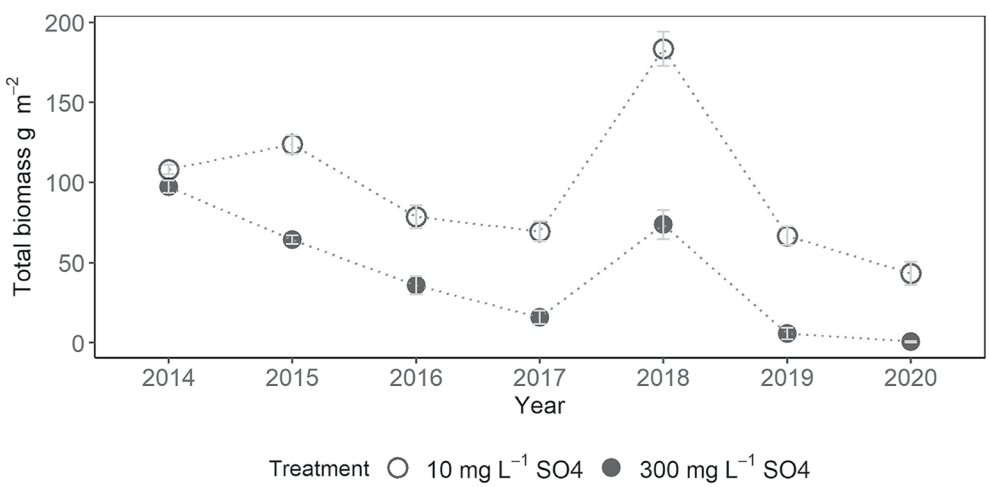

Figure 3. Annual average aboveground biomass (total) density (g m^{-2}) in populations grown in high sulfate (300 mg L^{-1}, filled circles) and low sulfate (10 mg L^{-1}, empty circles) in the overlying water. Error bars depict the standard error around the mean ($n = 20$).

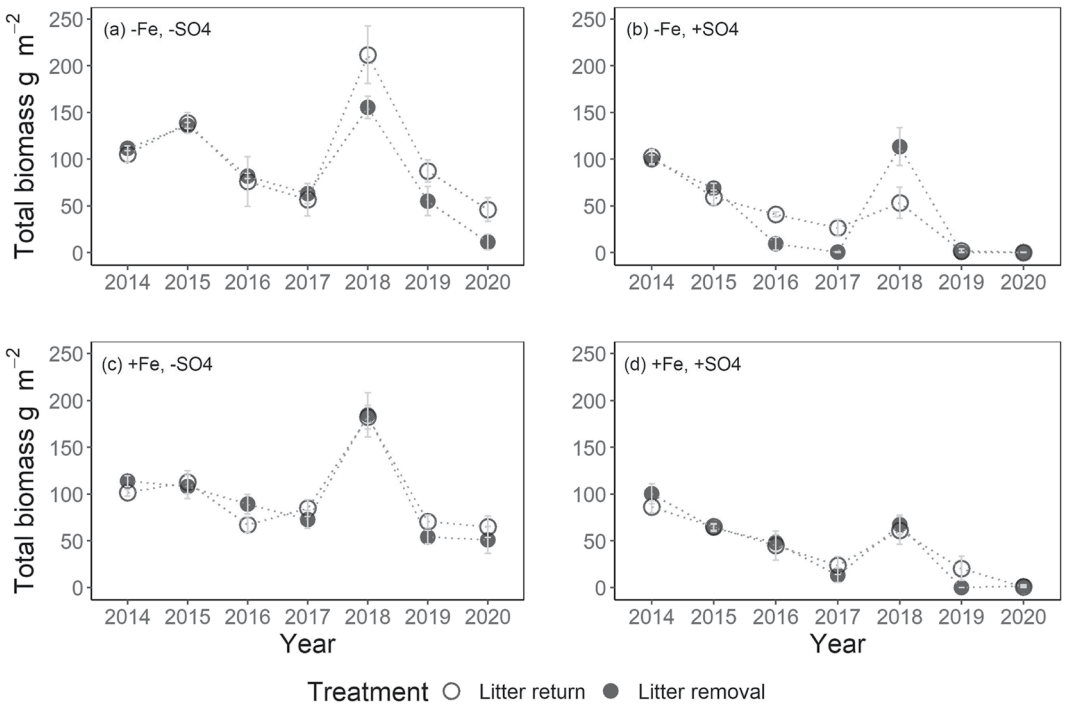

Figure 4. Annual average aboveground biomass (total) density (g m^{-2}) in populations grown with the previous year's aboveground litter returned (empty circles) or removed (filled circles). Populations were treated with combinations of low sulfate ($-SO_4$, 10 mg L^{-1}; a, c) or high sulfate ($+SO_4$, 300 mg L^{-1}; b, d) and low iron (−Fe, 4.3 mg g^{-1}; a, b) or high iron (+Fe, 10.9 mg g^{-1}; c, d). Error bars depict the standard error around the mean ($n = 5$).

conditions, populations showed a stable 3-year cycle of biomass (Figure 3) that oscillated between about 50 and 175 g m^{-2} on average, with peaks in the second and fifth growing season (2015 and 2018).

When biomass was examined separately in high-sulfate and low-sulfate treatments, populations grown in low sulfate were not affected by iron, litter, or their interaction (Figures 4a and 4c). Populations grown in high sulfate were not consistently influenced by iron and litter but were affected by interactions between iron, litter, and year (Table 3). In high-sulfate conditions, litter removal amplified oscillations in the treatments that did not receive iron addition, with lower biomass in years 3–4 of the experiment and higher biomass in year 5 compared to the populations with litter return (Figure 4b). In high-sulfate treatments that received additional iron, no differences in biomass were observed between litter removal and litter return (Figure 4d).

The proportion of filled seeds, individual seed mass, and population seed mass approached zero after six generations in high-sulfate conditions, while the same seed traits remained constant in low-sulfate conditions (Figure 5, seed mass not shown). Sulfate-amended populations that received iron amendment had a 20% higher filled seed ratio for 2015–2017 ($p = 0.01$, Table 3 and Figure 5b), but the effect of iron diminished in 2018 and 2019. In high-sulfate conditions, iron increased the average individual seed mass by approximately 40% in 2016 and by 20–30% in 2017–2018 ($p = 0.04$, Table 3 and Figure 5d). By 2020, only two sulfate-amended populations produced seeds; both also received iron amendment. In low-sulfate conditions, the proportion of filled seeds and average mass per filled seed were slightly increased by iron amendment (Figures 5a, 5c and Table 3). Litter removal did not affect any seed traits (Table 3).

3.3. Stability of Population Cycles

Changes in vegetative biomass from 1 year to the next were regressed against the biomass of the previous year to examine population oscillations for stability (Walker et al., 2010). All treatments with low sulfate were aggregated to compare to all treatments exposed to elevated sulfate since iron and litter manipulations had little effect in comparison to sulfate. In low-sulfate conditions, biomass oscillations are stable, as indicated by the slope of −1.3 for years 2015–2018 (Figure 6a) and a consistent annual biomass production between 50 and 125 g m^{-2}.

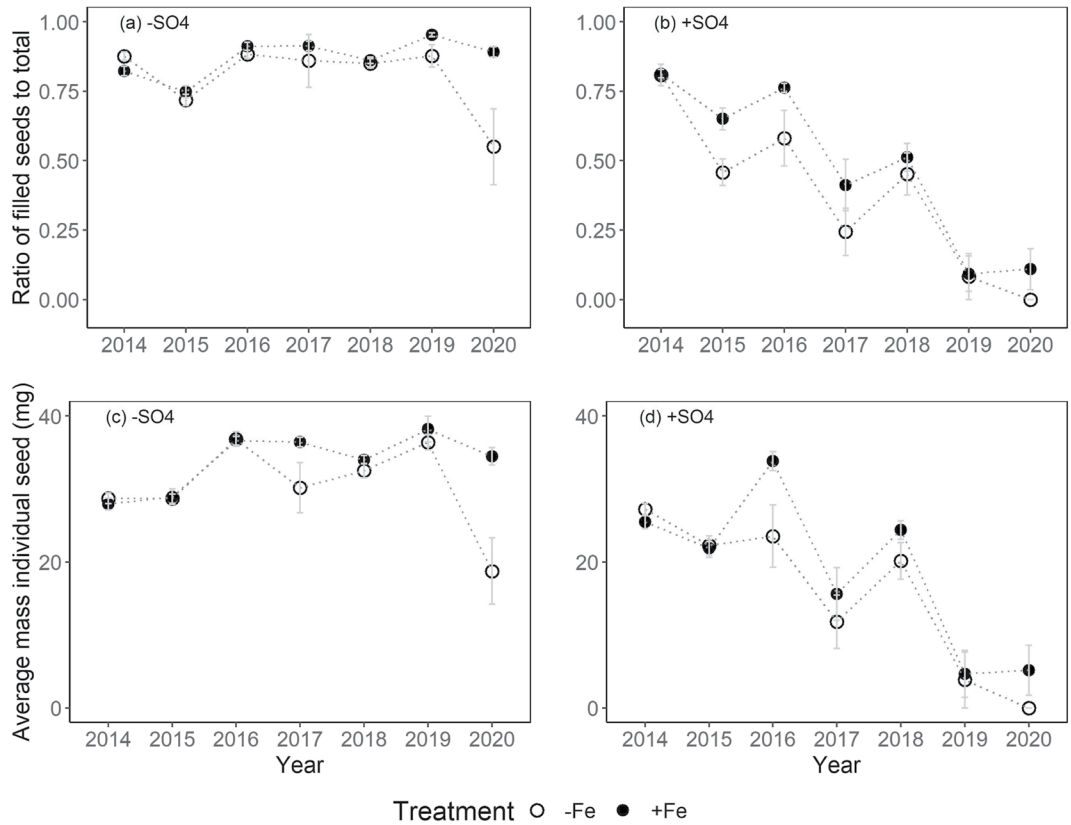

Figure 5. Effects of iron addition (+Fe, 10.9 mg g^{-1}; −Fe, 4.3 mg g^{-1}) on the ratio of filled seeds to total seeds (includes empty husks; a, b) and on average individual seed mass (c), (d) in 10 and 300 mg L^{-1} sulfate. Error bars depict the standard error around the mean ($n = 10$).

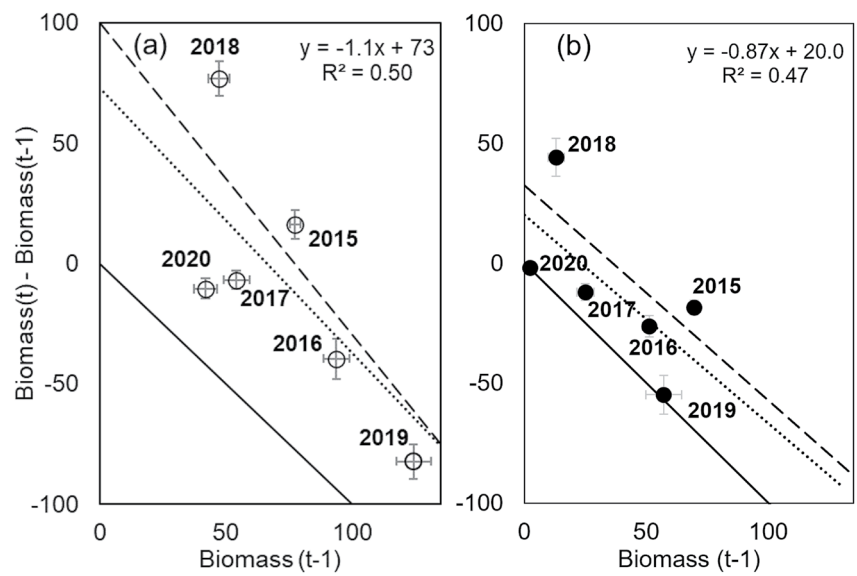

Figure 6. The relationship between average year-on-year change in vegetative biomass (g m^{-2}) to the previous year's vegetative biomass in (a) 10 mg L^{-1} sulfate and (b) 300 mg L^{-1} sulfate. Error bars show the standard error. The slope of the dashed line represents $\partial(dB/dt)/\partial B$ and is calculated from populations in 2015–2018, representing approximately one population cycle. The dotted line also represents $\partial(dB/dt)/\partial B$ and is calculated from 2015 to 2020, to show the stability after 1.5 population cycles. The solid line represents extinction, when all biomass from the previous year is lost.

This slope is nearly identical to the slopes found a previous experiment (−1.04 to −1.20) that showed wild rice undergoes litter-driven productivity cycles (Walker et al., 2010). When data from 2019 to 2020 are included in this analysis, the slope is −1.1, still representing stable oscillations. The present experiments and those of Walker et al. (2010) were done during different time periods and in different wild rice populations. Therefore, the two experiments provide independent corroboration of one another.

In high-sulfate conditions, a slope of −0.9 for year 2015–2018 indicates dampened oscillations (Figure 6b). Biomass decreased every year except for 2018, when the populations partially recovered. From 2018 to 2019, almost all points from sulfate-amended mesocosms fell on the boundary line $y = -x$, indicating that populations lost the entirety of the biomass produced during 2018 and produced no new biomass in 2019 (Figures 6b and 3). The data point for 2020 is near zero, indicating two consecutive years of extinct populations. The trajectory of mean biomass over time decreases in the presence of sulfate under our experimental conditions (Figure 3) and oscillations were dampened. In low-sulfate concentrations, biomass peaked in 2015 and 2018, demonstrating a 3-year cycle. Elevated sulfide produced in tanks with high-sulfate concentrations extinguished the population cycle which persisted in tanks with low-sulfate concentrations.

4. Discussion

Elevating surface water sulfate to 300 mg L^{-1} led mesocosm populations of wild rice to extinction in six growing seasons. This study adds to the growing body of literature describing the impacts of sulfate loading and subsequent sulfide exposure on wild rice, including lower rates of seedling survival, delayed phenology, impaired seed production, and declining biomass (Johnson et al., 2019; LaFond-Hudson et al., 2020a; Pastor et al., 2017). In conjunction, field observations both recently as well as decades ago show that wild rice presence becomes increasingly unlikely with elevated surface water sulfate and porewater sulfide (Moyle, 1945; Myrbo et al., 2017a). Statistical modeling of environmental parameters associated with wild rice presence has suggested that iron and organic carbon play the strongest role in controlling sulfide's effects on wild rice populations (Pollman et al., 2017), and similar conclusions have been reached about other sensitive aquatic plant species growing in freshwater wetlands with increasing sulfate loads (Lamers et al., 2002; Van der Welle et al., 2007). In our study, iron addition and organic carbon removal did not limit sulfide accumulation in sediment enough to stabilize wild rice populations.

In anoxic freshwater systems, sulfide production is generally limited by the supply of sulfate, whereas in marine systems or other systems with high sulfate, sulfide production is generally limited by the supply of organic matter (Ruiz-Halpern et al., 2008). Wild rice naturally grows in low-sulfate, organic-rich habitats (Myrbo et al., 2017a), meaning sulfate is the likely limiting factor for sulfide production. In mesocosms with elevated sulfate, litter removal alone did not appear to decrease sulfide concentrations and instead led to slightly faster population decline. It is possible that litter removal decreased the availability of macronutrients or micronutrients, such as nitrogen, potassium, or iron that might be replenished in natural ecosystems with more hydrologic connectivity. Notably, for populations with sulfate added and litter removed, population biomass declined faster in populations with ambient iron compared to populations receiving iron addition (Figures 4b and 4d). Another possibility is that in the litter return treatments, sulfate addition increased rates of litter decomposition and nutrient availability (Myrbo et al., 2017b). Under the conditions in this study and previous studies (Pastor et al., 2017), sulfide's inhibition of nitrogen uptake influenced population biomass more strongly than sulfate-enhanced nutrient mineralization, but the interactions of these two processes warrant further study.

In the presence of excess uncomplexed Fe(II), sulfide reacts quickly with iron, forming relatively stable iron sulfide solid phases. The ratio of sulfur to iron or similar metrics related to the degree of pyritization can be used to determine the capacity of sediment to precipitate iron sulfide and keep porewater sulfide concentrations low (Johnson et al., 2019; Julian et al., 2017). We added iron only during the first growing season of the experiment, making this treatment a pulse (one time) rather than a press (ongoing). In contrast, our sulfate and litter manipulations were maintained throughout the experiment. This decision was made to avoid Fe^{2+} toxicity to the plants (Kinsman-Costello et al., 2015; Sahrawat, 2005) and likely contributed to our findings of little alleviation of sulfide toxicity by iron compared to other studies with freshwater vegetation in environments with natural differences in groundwater upwelling of iron (Lamers et al., 2002) or seagrasses in experiments with monthly iron addition (Ruiz-Halpern et al., 2008). We observed some mitigation of sulfide's effects on seed production by

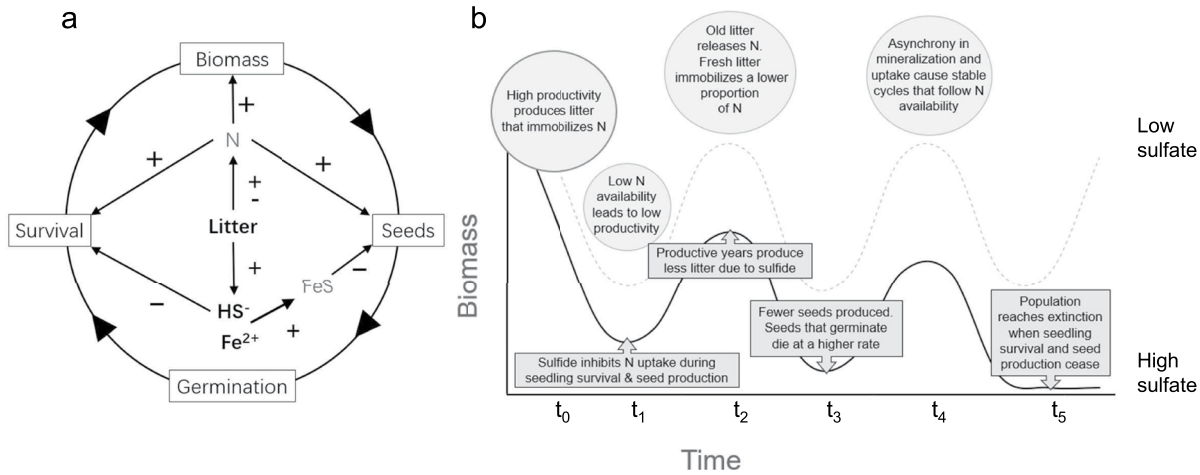

Figure 7. A conceptual model synthesizing the interactions of sulfur, iron, and litter during the life cycle of wild rice (a), and the effect of sulfur on interannual biomass cycles of wild rice (b) based on this study, Walker et al. (2010), and LaFond-Hudson et al. (2018). In (a), the (+) and (−) symbols in (a) represent positive or negative relationships between geochemical constituents and plant traits. In (b), the top, dashed line represents low-sulfate conditions, and the lower, solid line represents conditions with elevated sulfate loading. Time intervals ($t_0 - t_5$) do not represent consecutive years, because time between peaks is typically 3–5 years for wild rice.

iron in the first 4 years of the experiment, but iron's effect diminished by 2018 and 2019 (Figure 5) and porewater measurements in 2019 confirmed that iron concentrations were low in all elevated sulfate treatments, regardless of whether the mesocosms received additional iron (Figure 2).

The effect of sulfur on wild rice population dynamics is further complicated by oscillations due to a lag in nitrogen mineralization from litter relative to the timing of nitrogen uptake during the life cycle (Walker et al., 2010). We present a conceptual model built on the synthesis of previous work elucidating the connection between nitrogen and biomass cycles (Pastor & Walker, 2006; Walker et al., 2010); connections between sulfate, biomass, and seed production (Johnson et al., 2019; LaFond-Hudson et al., 2018; Pastor et al., 2017); and the present study which explores the role of sulfate and biomass cycles (Figure 7). Within each life cycle, nitrogen controls plant growth, and seed production (Grava & Raisanen, 1978). Litter immobilizes then slowly mineralizes nitrogen, leading to alternating negative and positive effects on nitrogen availability (Walker et al., 2010, Figure 7a). When sulfate is added to the system, production of sulfide directly decreases seedling survival and seed production (Figure 7a and Pastor et al., 2017). Iron precipitates sulfide into less-reactive iron sulfide, potentially alleviating some of the effects of sulfide on seedling survival and seed production, although iron sulfide also accumulates on root surfaces concomitant with decreased seed nitrogen (LaFond-Hudson et al., 2018). As the life cycle repeats each year (Figure 7a), these geochemistry-plant interactions lead to different interannual trajectories depending on the level of sulfate present in the system (Figure 7b). In low-sulfate conditions, high biomass production 1 year leads to an above average amount of litter that immobilizes nitrogen and decreases nitrogen availability in the following year(s) (Figure 7b, t_0, t_1). The lower nitrogen availability creates competition among seedlings for scarce nitrogen, leading to diminished biomass and seed production. As litter slowly decays, it releases nitrogen during subsequent years (Figure 7b t_2), and thereby increases seedling survival, biomass, and seed production. Alternating nitrogen availability leads to stable biomass cycles in low-sulfate environments (Figures 3 and 7b, t_4 etc.). At the levels of experimental sulfate addition we used, sulfur impacts overwhelmed the effects of litter-controlled N availability, causing the populations to quickly decrease (Figures 3 and 7b, t_3). When constant sulfate loading sustains declines in seedling survival and seed production, both germination and population biomass decline, eventually to extinction (Figure 7b, t_5).

Although we examined complicated interactions among sulfur, iron, organic carbon, nitrogen, and plant cycles, the mesocosms we used in this study are a relatively simple system containing only one species, homogenized sediment across mesocosms, and little hydrological mixing or external nutrient inputs. Projects that manage or restore plant populations in aquatic ecosystems occur in systems affected by interactions between geochemistry, surface and groundwater hydrology, and competing ecological communities. Many such projects monitor biomass annually, but traditional time series analyses require lengthy monitoring periods. When the monitoring period is

too short to detect population oscillations with a time series analysis, it may be insightful to use annual biomass data from one or two population cycles to calculate and analyze eigenvalues that describe the population's stability. In our experiment, we calculated and analyzed eigenvalues from less than two population cycles and our eigenvalue for populations in low-sulfate conditions corresponded closely to the results of Walker et al. (2010). Even though these were different experiments done during nonoverlapping time periods, the two experiments corroborate one another and strongly suggest that wild rice populations unimpeded by sulfate loadings oscillate stably with an approximate period of 4 years. Additionally, these findings are consistent with observations in some regional lakes and rivers containing wild rice stands (Vogt, 2021). This method is general enough to be applied analogously to data from other field studies and may be useful for identifying at-risk populations or determining whether management and restoration of an oscillating population is effective.

Only some aquatic plants experience population oscillations; however, many are limited by nitrogen and experience sustained or occasional exposure to sulfide, for example, the salt marsh species *Spartina alterniflora* (Mendelssohn & Morris, 2000). Estuarine wetlands receive sulfate from tidal inputs and interannual changes in precipitation can lead to wide variations in interannual nitrogen loading and sulfate intrusion (Sinha & Michalak, 2016). Understanding how plants respond to sulfate and sulfide under fluctuating nitrogen availability may be critical for understanding wetland vegetation dynamics. Perhaps species with different patterns of nitrogen uptake compared to wild rice can be more resilient to sulfide exposure, or plants with greater sulfide tolerance benefit more from increased sulfur-mediated nutrient availability.

5. Conclusion

This study demonstrates the importance of both litter-driven biomass oscillations and sulfate concentrations to population trajectories over several generations and corroborates studies that investigated these processes separately (Johnson et al., 2019; Pastor et al., 2017; Walker et al., 2010). Our observations show predictable and stable biomass oscillations in systems with less than 10 mg L^{-1} sulfate in surface water and rapid population declines in systems with surface water sulfate elevated to 300 mg L^{-1}. Although population biomass did oscillate in elevated sulfate conditions, oscillations were unstable and less predictable than in low-sulfate conditions. This work aggregates well-understood rhizosphere and geochemical processes to interpret the effects realized at a population scale. We did not find consistent or sustained contributions of iron or litter to stability of wild rice populations. Instead, interactions between sulfate, litter, and iron in this study point to complex couplings among plant life cycles, nutrient availability, and iron and sulfur cycling that become manifest over several generations through at least one population cycle. We conclude that both geochemical context and plant life cycle patterns play a considerable role in determining the stability of oscillating plant populations.

Conflict of Interest

The authors declare no conflicts of interest relevant to this study.

Data Availability Statement

Data are publicly available at the Digital Repository for University of Minnesota at https://doi.org/10.13020/cq0g-r486 and are cited within the data analysis section of the methods.

Acknowledgments
This work was prepared by S. LaFond-Hudson, N. Johnson, J. Pastor, and B. Dewey using federal funds under award NA15OAR4170080 from Minnesota Sea Grant, National Sea Grant College Program, National Oceanic and Atmospheric Administration, U.S. Department of Commerce. The statements, findings, conclusions, and recommendations are those of the author(s) and do not necessarily reflect the views of NOAA, the Sea Grant College Program, or the U.S. Department of Commerce. The authors would like to thank the Fond du Lac Band of Lake Superior Chippewa for providing sediment. This manuscript has been authored by UT-Battelle, LLC under Contract No. DE-AC05-00OR22725 with the U.S. Department of Energy. The United States Government retains and the publisher, by accepting the article for publication, acknowledges that the United States Government retains a nonexclusive, paid-up, irrevocable, world-wide license to publish or reproduce the published form of this manuscript, or allow others to do so, for United States Government purposes. The Department of Energy will provide public access to these results of federally sponsored research in accordance with the DOE Public Access Plan (http://energy.gov/downloads/doe-public-access-plan).

References

Azam, F., Lodhi, A., & Ashraf, M. (1991). Availability of soil and fertilizer nitrogen to wetland rice following wheat straw amendment. *Biology and Fertility of Soils*, *11*, 97–100. https://doi.org/10.1007/BF00336371

Bailey, L. T., Mitchell, C. P. J., Engstrom, D. R., Berndt, M. E., Coleman Wasik, J. K., & Johnson, N. W. (2017). Influence of porewater sulfide on methylmercury production and partitioning in sulfate-impacted lake sediments. *Science of The Total Environment*, *580*, 1197–1204. https://doi.org/10.1016/j.scitotenv.2016.12.078

Blossfeld, S., Gansert, D., Thiele, B., Kuhn, A. J., & Lösch, R. (2011). The dynamics of oxygen concentration, pH value, and organic acids in the rhizosphere of Juncus spp. *Soil Biology and Biochemistry*, *43*, 1186–1197. https://doi.org/10.1016/j.soilbio.2011.02.007

Federation, W. E., & Association, A. P. H. (2005). *Standard methods for the examination of water and wastewater*. American Public Health Association, American Water Works Association, Water Environment Federation.

Fond du Lac Band of Lake Superior Chippewa. (2018). Expanding the narrative of tribal health: The effects of wild rice water quality rule changes on tribal health (Vol. *68*). Health Impact Assessment.

Gao, S., Tanji, K., & Scardaci, S. (2003). Incorporating straw may induce sulfide toxicity in paddy rice. *California Agriculture*, *57*, 55–59. https://doi.org/10.3733/ca.v057n02p55

Gao, S., Tanji, K. K., & Scardaci, S. C. (2004). Impact of rice straw incorporation on soil redox status and sulfide toxicity. *Agronomy Journal*, *96*, 70–76. https://doi.org/10.2134/agronj2004.7000

Grava, J., & Raisanen, K. A. (1978). Growth and nutrient accumulation and distribution in wild rice 1. *Agronomy Journal*, *70*, 1077–1081. https://doi.org/10.2134/agronj1978.00021962007000060044x

Han, C., Ren, J., Wang, Z., Yang, S., Ke, F., Xu, D., & Xie, X. (2018). Characterization of phosphorus availability in response to radial oxygen losses in the rhizosphere of Vallisneria spiralis. *Chemosphere*, *208*, 740–748. https://doi.org/10.1016/j.chemosphere.2018.05.180

Hildebrandt, L. R., Pastor, J., & Dewey, B. (2012). Effects of external and internal nutrient supplies on decomposition of wild rice, *Zizania palustris*. *Aquatic Botany*, *97*, 35–43. https://doi.org/10.1016/j.aquabot.2011.11.002

Johnson, N. W., Pastor, J., & Swain, E. B. (2019). Cumulative sulfate loads shift porewater to sulfidic conditions in freshwater wetland sediment. *Environmental Toxicology and Chemistry*, *38*, 1231–1244. https://doi.org/10.1002/etc.4410

Jorgenson, K. D., Lee, P. F., & Kanavillil, N. (2012). Ecological relationships of wild rice, *Zizania* spp. 11. Electron microscopy study of iron plaques on the roots of northern wild rice (*Zizania palustris*). *Botany*, *91*, 189–201. https://doi.org/10.1139/cjb-2012-0198

Julian, P., Chambers, R., & Russell, T. (2017). Iron and pyritization in wetland soils of the Florida Coastal Everglades. *Estuaries and Coasts*, *40*, 822–831. https://doi.org/10.1007/s12237-016-0180-3

Kinsman-Costello, L. E., O'Brien, J. M., & Hamilton, S. K. (2015). Natural stressors in uncontaminated sediments of shallow freshwaters: The prevalence of sulfide, ammonia, and reduced iron. *Environmental Toxicology and Chemistry*, *34*, 467–479. https://doi.org/10.1002/etc.2801

LaFond-Hudson, S., Johnson, N. W., Pastor, J., & Dewey, B. (2018). Iron sulfide formation on root surfaces controlled by the life cycle of wild rice (*Zizania palustris*). *Biogeochemistry*, *141*, 95–106. https://doi.org/10.1007/s10533-018-0491-5

LaFond-Hudson, S., Johnson, N. W., Pastor, J., & Dewey, B. (2020a). Interactions between sulfide and reproductive phenology of an annual aquatic plant, wild rice (*Zizania palustris*). *Aquatic Botany*, *164*, 103230. https://doi.org/10.1016/j.aquabot.2020.103230

LaFond-Hudson, S., Johnson, N. W., Pastor, J., & Dewey, B. (2020b). *Supporting data for "Sulfur geochemistry impacts population oscillations of wild rice (Zizania palustris)* (Data Repository). University of Minnesota. https://doi.org/10.13020/cq0g-r486

Lamers, L. P. M., Falla, S.-J., Samborska, E. M., van Dulken, I. A. R., van Hengstum, G., & Roelofs, J. G. M. (2002). Factors controlling the extent of eutrophication and toxicity in sulfate-polluted freshwater wetlands. *Limnology & Oceanography*, *47*, 585–593. https://doi.org/10.4319/lo.2002.47.2.0585

Lamers, L. P. M., Govers, L. L., Janssen, I. C., Geurts, J. J., Van der Welle, M. E., Van Katwijk, M. M., et al. (2013). Sulfide as a soil phytotoxin—A review. *Frontiers of Plant Science*, *4*, 268. https://doi.org/10.3389/fpls.2013.00268

Lawrence, M. (2016). ez [WWW Document]. Retrieved from https://cran.r-project.org/web/packages/ez/ez.pdf

Lee, P. F. (2002). Ecological relationships of wild rice, *Zizania* spp. 10. Effects of sediment and among-population variations on plant density in *Zizania palustris*. *Canadian Journal of Botany*, *80*, 1283–1294. https://doi.org/10.1139/b02-118

Marzocchi, U., Benelli, S., Larsen, M., Bartoli, M., & Glud, R. N. (2019). Spatial heterogeneity and short-term oxygen dynamics in the rhizosphere of Vallisneria spiralis: Implications for nutrient cycling. *Freshwater Biology*, *64*, 532–543. https://doi.org/10.1111/fwb.13240

Mendelssohn, I. A., Kleiss, B. A., & Wakeley, J. S. (1995). Factors controlling the formation of oxidized root channels: A review. *Wetlands*, *15*, 37–46. https://doi.org/10.1007/BF03160678

Mendelssohn, I. A., & Morris, J. T. (2000). Eco-physiological controls on the productivity of *Spartina alterniflora* Loisel. In M. P. Weinstein, & D. A. Kreeger (Eds.), *Concepts and controversies in tidal marsh ecology* (pp. 59–80). Springer. https://doi.org/10.1007/0-306-47534-0_5

Morse, J. W., Millero, F. J., Cornwell, J. C., & Rickard, D. (1987). The chemistry of the hydrogen sulfide and iron sulfide systems in natural waters. *Earth-Science Reviews*, *24*, 1–42. https://doi.org/10.1016/0012-8252(87)90046-8

Moyle, J. B. (1945). Some chemical factors influencing the distribution of aquatic plants in Minnesota. *The American Midland Naturalist*, *34*, 402–420. https://doi.org/10.2307/2421128

Myrbo, A., Swain, E. B., Engstrom, D. R., Wasik, J. C., Brenner, J., Shore, M. D., et al. (2017a). Sulfide generated by sulfate reduction is a primary controller of the occurrence of wild rice (*Zizania palustris*) in shallow aquatic ecosystems. *Journal of Geophysical Research: Biogeosciences*, *122*, 2736–2753. https://doi.org/10.1002/2017JG003787

Myrbo, A., Swain, E. B., Johnson, N. W., Engstrom, D. R., Pastor, J., Dewey, B., et al. (2017b). Increase in nutrients, mercury, and methylmercury as a consequence of elevated sulfate reduction to sulfide in experimental wetland mesocosms: SO_4 reduction mobilizes N, P, C, and mercury. *Journal of Geophysical Research: Biogeosciences*, *122*, 2769–2785. https://doi.org/10.1002/2017JG003788

Pastor, J., Dewey, B., Johnson, N. W., Swain, E. B., Monson, P., Peters, E. B., & Myrbo, A. (2017). Effects of sulfate and sulfide on the life cycle of *Zizania palustris* in hydroponic and mesocosm experiments. *Ecological Applications*, *27*, 321–336. https://doi.org/10.1002/eap.1452

Pastor, J., & Walker, R. D. (2006). Delays in nutrient cycling and plant population oscillations. *Oikos*, *112*, 698–705. https://doi.org/10.1111/j.0030-1299.2006.14478.x

Pollman, C. D., Swain, E. B., Bael, D., Myrbo, A., Monson, P., & Shore, M. D. (2017). The evolution of sulfide in shallow aquatic ecosystem sediments: An analysis of the roles of sulfate, organic carbon, and iron and feedback constraints using structural equation modeling. *Journal of Geophysical Research: Biogeosciences*, *122*, 2719–2735. https://doi.org/10.1002/2017JG003785

Ruiz-Halpern, S., Macko, S. A., & Fourqurean, J. W. (2008). The effects of manipulation of sedimentary iron and organic matter on sediment biogeochemistry and seagrasses in a subtropical carbonate environment. *Biogeochemistry*, *87*, 113–126. https://doi.org/10.1007/s10533-007-9162-7

Sahrawat, K. L. (2005). Iron toxicity in wetland rice and the role of other nutrients. *Journal of Plant Nutrition*, *27*, 1471–1504. https://doi.org/10.1081/PLN-200025869

Sain, P. (1984). Decomposition of wild rice (*Zizania aquatica*) straw in two natural lakes of northwestern Ontario. *Canadian Journal of Botany*, *62*, 1352–1356. https://doi.org/10.1139/b84-183

Sims, L., Pastor, J., Lee, T., & Dewey, B. (2012). Nitrogen, phosphorus and light effects on growth and allocation of biomass and nutrients in wild rice. *Oecologia*, *170*, 65–76. https://doi.org/10.1007/s00442-012-2296-x

Sinha, E., & Michalak, A. M. (2016). Precipitation dominates interannual variability of riverine nitrogen loading across the continental United States. *Environmental Science & Technology*, *50*, 12874–12884. https://doi.org/10.1021/acs.est.6b04455

Strogatz, S. H. (1994). *Nonlinear dynamics and chaos: With applications to physics, biology, chemistry, and engineering*. Westview Press.

Sundby, B., Vale, C., Caçador, Z., Catarino, F., Madureira, M.-J., & Caetano, M. (1998). Metal-rich concretions on the roots of salt marsh plants: Mechanism and rate of formation. *Limnology & Oceanography*, *43*, 245–252. https://doi.org/10.4319/lo.1998.43.2.0245

Van der Welle, M. E. W., Niggebrugge, K., Lamers, L. P. M., & Roelofs, J. G. M. (2007). Differential responses of the freshwater wetland species Juncus effusus L. and Caltha palustris L. to iron supply in sulfidic environments. *Environmental Pollution*, *147*, 222–230. https://doi.org/10.1016/j.envpol.2006.08.024

Vogt, D. (2021). *Wild rice monitoring and abundance in the 1854 Ceded Territory (199–2020)* (Tech. Rep. 1854). Treaty Authority.

Walker, R., Pastor, J., & Dewey, B. W. (2006). Effects of wild rice (*Zizania palustris*) straw on biomass and seed production in northern Minnesota. *Canadian Journal of Botany*, *84*, 1019–1024. https://doi.org/10.1139/b06-058

Walker, R. E. D., Pastor, J., & Dewey, B. W. (2010). Litter quantity and nitrogen immobilization cause oscillations in productivity of wild rice (*Zizania palustris* L.) in northern Minnesota. *Ecosystems*, *13*, 485–498. https://doi.org/10.1007/s10021-010-9333-6